The Effects of NAD-Boosting Therapies on Sirtuin Activity and DNA Repair Capacity

The Effects of NAD-Boosting Therapies on Sirtuin Activity and DNA Repair Capacity

Colleen E. Kelley

A Thesis in the Field of Biotechnology

for the Degree of Master of Liberal Arts in Extension Studies

Harvard University

May 2020

Abstract

As we age, we accumulate DNA damage that results in the chronic activation of PARP, a critical enzyme involved in the DNA repair process (Mouchiroud et al. 2013; Gomes et al. 2013; Yoshino et al. 2013). Chronic activation of PARP leads to an age-associated decline of nicotinamide adenine dinucleotide (NAD) and an increase in nicotinamide (NAM), which inhibits critical enzymes such as the sirtuins, nicotinamide phosphoribosyl transferase (NAMPT), and even PARP itself (Gomes et al. 2013; Zhu et al. 2015; Zhang et. al. 2016). As a result, increased levels of PARP have been observed in many chronic diseases such as diabetes, cancer, and neurodegenerative diseases (Love et al. 1999; Kauppin and Swanson 2007; Pacher and Szabo 2005; Peralta-Leal et al. 2009). We were able to detect the upregulation of PARP and inhibition of the sirtuins in the tissues of aged mouse kidneys. We then developed a DNA damage *in vitro* model that mimics the increase of DNA damage markers that we observed in aged animals. In this model, we were able to demonstrate that DNA damage drives an increase in markers associated with senescence, inflammation, and fibrosis. This correlates with published literature surrounding the development of age-associated diseases as well as the occurrence of radiation-induced fibrosis in cancer patients (Serrano et al. 2014; Straub et al. 2016). Recent studies in mouse *in vivo* models have shown the benefits of using NAD-boosting therapies to improve or delay the onset of many age-associated diseases (Belenky et al. 2007; Balan et al. 2008; Mouchiroud et al. 2013). We were able to compare supplementation of a NAD precursor, Nicotinamide Riboside (NR), with P7C3, a known NAMPT activator, in our *in vitro* DNA damage model. We observed that P7C3

was superior to NR to alleviate markers associated with DNA damage, senescence, inflammation and fibrosis in the context of increased DNA damage.

Acknowledgments

I would not have been able to complete this work without the help of my thesis directors, Jeff Hewett and Dr. Christy Fryer. I am so appreciative of your encouragement, support, and feedback throughout my thesis project.

Thank you to Dr. Jim Morris, my thesis adviser, who has been a helpful guide and reference throughout this entire thesis development process.

Finally, thanks to my husband, Jon, for supporting me on this long journey to complete my Master's Degree. Without your patience and encouragement through late nights, statistics tutoring, and hours of being my sounding board, I would not have been able to do this without you.

Table of Contents

List of Figures and Graphs

Chapter I

Introduction

It has been well documented that DNA damage accumulation with age or pathology leads to development of chronic inflammation, fibrosis, and eventual decline in tissue function (Lopez-Otin et. al. 2012; Serrano et. al. 2014; Vijg et. al. 2017). In normal healthy tissue, cells that are exposed to DNA damage undergo senescence where they stop dividing and trigger the release of cytokines and other pro-inflammatory signals. This senescent-associated secretory phenotype (SASP) response acts as a signal to recruit macrophages directly to senescent cells, allowing these cells to be cleared and the damaged tissue to regenerate (Campisi 2013; Kuilman and Peeper 2009). However, upon persistent damage, age, or disease, senescent cells accumulate more quickly than they can be cleared, resulting in the chronic upregulation of inflammation and eventual development of fibrosis in damaged tissue (Munoz-Espin and Serrano 2014) (Figure 1). Therefore, efforts to improve DNA repair capacity and target senescent cells have exhibited therapeutic potential to delay the onset of fibrosis and other age-associated diseases.

Why NAD?

Many reports link the accumulation of DNA damage to an age-related decline in nicotinamide adenine dinucleotide (NAD) levels (Gomes et. al. 2013; Zhu et. al. 2015;

Zhang et. al. 2016). While NAD is known as an essential cofactor that drives cellular metabolism, it is also the substrate for key enzymes involved in the DNA repair process, the PARPs and sirtuins. These NAD-consuming enzymes play a vital role in many biological processes, including maintaining genomic stability, mitochondrial metabolism, and stress resistance (Lopez-Otin et. al. 2012; Vijg et. al. 2017). Due to the integral role of these enzymes in improving life and health span, many recent studies have shown the benefits of using NAD-boosting therapies to activate these enzymes as a means to delay the onset of aging and age-related disorders (Belenky et. al. 2007; Balan et. al. 2008; Mouchiroud et. al. 2013).

NAD is primarily synthesized through the NAD-salvage pathway through its precursors: nicotinic acid (NA), nicotinamide (NAM), nicotinamide mononucleotide (NMN), and nicotinamide riboside (NR) (Hottiger and Hassa 2008). Once NAD is generated in the cell, it is consumed by both sirtuins and PARPs, releasing NAM as a byproduct (Hottiger and Hass 2008; Fang et. al. 2016). Upon persistent DNA damage with age, PARP enzymes become chronically upregulated leading to a depletion of NAD and an increase in levels of NAM (Mouchiroud et al. 2013; Gomes et al. 2013; Yoshino et al. 2013). As a result, the imbalance of NAD and NAM levels has been shown to inhibit SIRT1 through competitive binding between NAD and NAM at a particular binding pocket on SIRT1 (Bitterman et. al. 2002). Therefore, it is believed that boosting levels of NAD would restore the substrate required for the sirtuins and PARPs to maintain their role as guardians of the genome.

The Role of Sirtuins on DNA Repair and Maintenance

The sirtuins are a family of histone deacetylases (HDACs) that consume NAD in order to regulate the activity of target proteins involved in essential cellular processes. There are seven known sirtuins. They all share a common core domain, but differ structurally on their N and C terminus (Frye et al. 2000). They also differ in their sub-cellular localization, which allows the sirtuins to have both unique and overlapping protein targets as well as biological functions. SIRT1, the most well studied sirtuin, is located in the nucleus and is known to target important proteins involved in cellular stress response (e.g. p53, Nf-κB, and PARP1) and mitochondrial health (e.g. PGC1α) (Meyer at al. 2017; Yeung et al. 2004); Vaziri et al. 2001; Rodgers et al. 2005) . SIRT2 is located in the cytoplasm and has been reported to regulate gene expression by deacetylating transcriptional regulators (North et al. 2007). SIRT3, 4, and 5 are all located in the mitochondria and play an integral role in oxidative stress (Ahuja et al. 2007; Jeong et al. 2013; Zhang et al. 2015; Rardin et al. 2013). Finally, SIRT6 and 7 are nuclear sirtuins. SIRT6 in the only reported sirtuin to increase lifespan in mice and has shown to play a vital role in heterochromatin maintenance and DNA repair capacity (Mao et al. 2011).

The plethora of data surrounding the benefits of sirtuin gain of function and activation on many metabolic and age-related disorders has reignited interest in NAD and potential therapies that could boost NAD levels. As previously stated, NAD is primarily synthesized through the salvage pathway by its precursors NA, NMN, and NR (Hottiger and Hassa 2008). NA has been reported to increase NAD levels and improve genome stability in mice (Burkle et al. 2017). However, patients administered NA for the

treatment of cardiovascular diseases experienced uncomfortable flushing (Altschul et al. 1955). NMN has also been shown to activate SIRT1 and long-term administration mitigates an age-associated decline in energy metabolism, lipid metabolism, and insulin sensitivity (Mills et al. 2016). However, NMN must first be converted to NR through a dephosphorylation step that is executed by NRK1/2 in order to enter the cell and then converted back to NMN to be utilized in the NAD salvage pathway (Belenky et al. 2007) (Figure 2). Therefore, one of the most promising reported NAD-boosting therapies is the direct administration of NR.

NR as a potential therapy for Age-Related Disorders

The number of studies investigating NR supplementation as an effective NAD-boosting therapy has grown rapidly. The only FDA approved supplement of NR, known as Niagen®, is owned by ChromaDex Inc. and its benefits are currently being assessed through human clinical trials for diabetic neuropathy, heart failure, hypertension, concussions, and other various age-related indications. ChromaDex claims that Niagen® can restore NAD levels in the human body after only 8 weeks of administration and recently sponsored a study with the National Institute on Aging for Niagen® administration in a mouse model for Cockayne Syndrome (CS) (Bohr et. al. 2014). While metabolic deficiencies associated with accumulated DNA damage typically occur over decades, patients with CS lack normal DNA repair machineries causing them to display signs of premature aging and a shortened lifespan. In this mouse study, NR treatment was reported to boost NAD and ATP levels and restore RNA transcription

compared to untreated CS mice (Bohr et al. 2014). Numerous other publications have also described the beneficial effects of NR treatment, particularly in animal models for type II diabetes, hearing loss, cardiac injury, and muscle degeneration (Canto et al. 2012; Brown et al. 2014; Trammel et al. 2016; Ryu et al. 2016) . While the results in these age-related indications look incredibly promising, there is a lack of data demonstrating a direct link between NR supplementation to sirtuin activation and improved DNA repair capacity.

P7C3 as an Alternative to NAD precursors

In addition to supplementation with a NAD precursor, pharmacological intervention with small molecules have proven to be an alternative approach to boost NAD levels. In an attempt to find a novel neuroprotective small molecule, McKnight et. al. discovered P7C3-A20, an aminopropyl carbazole that exhibited beneficial effects in a rodent model of Parkinson's disease (Pieper, A.A. et. al. 2014). Upon further investigation, McKnight's team discovered that the target of P7C3-A20, was nicotinamide phosphoribosyl transferase (NAMPT), the rate limiting enzyme in the NAD salvage pathway (McKnight et. al. 2014). NAMPT is responsible for generating NMN from NAM, thereby playing a predominant role in maintaining NAD levels (Figure 2). Quickly after its discovery, P7C3-A20 was reported to increase NAD levels and protect against doxorubicin-induced DNA damage in cells (Wang et. al. 2014). Administration of P7C3-A20 in rodents exhibited pro-neurogenic and neuroprotective effects on mature neurons (Wang et. al. 2018; Wang et. al. 2017). Additionally, treatment with this small

molecule has shown a protective benefit in rodents against spinal cord injury and ischemic stroke as well as antidepressant effects by increasing hippocampal neurogenesis (Miao et. al. 2016; Hu et. al. 2019; Zigman et. al. 2015). Therefore, treatment with P7C3-A20 could prove to be a potential therapy to protect against DNA damage and delay the onset of various age-related disorders.

Research Aims, Goals, and Hypothesis

The goal of our study is to compare mechanisms of NAD-boosting therapies to improve DNA repair capacity and counter regulate markers associated with disease progression in age. We hypothesize that, in the context of DNA damage, NR and P7C3 administration can increase NAD levels, resulting in SIRT activation, improvement in DNA repair capacity, and modulation of markers associated with DNA damage, senescence, inflammation, and fibrosis.

Specific Aim 1: Assess the activity of DNA repair enzymes and dysregulation of metabolites associated with the NAD salvage pathway in the tissues of young and aged animals.

Methods: Monitor differences in post-translational modifications of DNA repair enzymes by western blot and measure age-associated metabolite changes in the NAD salvage pathway.

Expected Results: There will be a decrease in the activity of DNA repair enzymes resulting in DNA damage accumulation as well as an imbalance in metabolites associated with the NAD salvage pathway.

Specific Aim 2: Compare whether NR and P7C3 can modulate the activities of DNA repair enzymes, improve DNA repair capacity, and counter regulate genes associated with senescence, inflammation, and fibrosis in the context of DNA damage *in vitro*.

Methods: Monitor differences in post-translational modifications of DNA repair enzymes by western blot and transcriptional changes of pathways related to DNA repair capacity by RT-qPCR.

Expected Results: Both NAD-boosting therapies will activate the sirtuins and improve DNA repair capacity in the context of DNA damage.

Chapter II

Materials and Methods

Animals

Two sets of animal cohorts were used in this study. The first animal cohort consisted of a total of 16 C57BL/6N mice aged 6 and 27 months (n=8 per group) from Jackson Laboratories and were used for western blots and metabolite analysis. The second animal cohort consisted of 15 C57BL/6J mice aged 6 and 24 months (n=8 and 7, respectively) from Jackson Laboratories and were used for metabolite analysis. The kidneys from both cohorts were dissected and flash frozen in liquid nitrogen upon takedown. Samples were stored at -80°C until use. Kidney samples were pulverized in liquid nitrogen by mortar and pestle into a fine, homogenous powder and stored at -80°C.

Western Blot Analysis of Aged Mouse Kidneys

For protein extractions, 30mg of pulverized mouse kidney samples were weighed in 1.5mL Precellys® tubes with 1.4mm beads and homogenized at 4°C in RIPA lysis buffer with Halt® Protease and Phosphatase inhibitor cocktail (Thermo Fisher Scientific, MA). Following a 30-minute incubation at 4°C, protein lysates were microcentrifuged in 1.5mL Eppendorf® tubes and the supernatants were collected for protein analysis. Protein concentrations were determined by a bicinchoninic acid (BCA) protein assay

(Thermo Fisher Scientific, MA). Diluted proteins were separated by SDS-PAGE using a 4-20% Criterion TGX Precast Midi Protein Gel (Bio-Rad, CA) and transferred to a nitrocellulose membrane by use of a Trans Turbo Blot system (Bio-Rad). Membranes were blocked with 5% milk in Tris-buffered saline with Tween-20® (TBS-T) for 1 hour at room temperature and were incubated with primary antibodies overnight at 4°C. The following day, membranes were washed three times with TBS-T and incubated with the appropriate HRP-conjugated secondary antibodies (Thermo Fisher Scientific) for 1 hour at room temperature. The following primary antibodies were used at a 1:1000 dilution: GAPDH (Cell Signaling #2188S), Acetyl-P53 (K382) (Thermo #710294), PAR (ENZO #BML-SA216-0100), and PARP (Cell Signaling #9542S). The following secondary antibodies (Thermo Fisher Scientific) were used at a 1:5000 dilution: Goat anti-Mouse IgG (H+L) Secondary Antibody, HRP (#31430) and Goat anti-Rabbit (H+L) Secondary Antibody, HRP (#31460).

Metabolite Analysis in Young and Old Mouse Kidneys

For metabolite analysis, 5-10mg of young and old mouse kidney tissue were weighed in 1.5mL Precellys® tubes with 1.4mm beads and homogenized at 4°C in 400ul of cold 80:20 Methanol/Water by use of a Precellys® 24 Tissue Homogenizer (Bertin Instruments, France). After homogenization, the samples were frozen overnight at -80°C. The following day, the samples were transferred to a 1.5mL Eppendorf® tube, micro-centrifuged at 4°C at 12,000 rpm for 15 minutes, and supernatants containing metabolites were transferred to a 96 well plate for Mass Spectrometry analysis.

Equal volume of internal standards were added to each sample. In this study, the internal standard solution was a methanol solution of stable isotope labeled NAM and NAD (0.2 μM each). Depending on the sample concentrations, 0.5 to 1 μL of the sample and internal standard mixed solution were injected into a LC/MS system that is composed of an LC (iClass UPLC from Waters) coupled to a mass spectrometer (6500 QTrap from AB Sciex). The separation was carried out in a HILIC mode using a 150x2.1mm column (ZIC HILIC from Merck Sequent). A binary gradient was used for elution with acetonitrile and 10mM ammonium acetate in water added with acetic acid to 0.1% (v/v). The mass spectrometry detection and quantification used multiple reaction monitoring. NAD and NAM were identified by matching retention time with their corresponding heavy isotope labeled standards and absolute concentrations were quantified when possible. For all other metabolites, signals were normalized to heavy isotope labeled NAD. No attempts were made to calculate absolute concentrations.

DNA Damage induced in-vitro validation

In order to determine the IC50 of Doxorubicin in U2OS cells, U2OS cells (ATCC, VA) were plated at 2,000 cells/well in a 384-well white plate (Thermo Fisher Scientific). The next day, cells were dosed in triplicate at a starting final concentration of 50μM in a 16-point dose response by use of an Echo Acoustic Liquid Handling Dispenser (Labcyte Inc, CA). Treated cells were incubated for 72 hours. Cell viability was determined using a Cell Titer Glo® readout (Promega, WI) by an Envision® Plate Reader (PerkinElmer, MA) for luminescence.

For western and RT-qPCR assays, U2OS cells were plated on 10cm plates at 1.3 x 10^6 cells per well. The following day, cells were dosed with 0.5μM of Doxorubicin (Tocris Bioscience #25316-40-9) either alone or in combination with Nicotinamide Riboside (Cayman Chemical #23132), P7C3-A20 (Novartis), Ex527 (Sigma #E7034), or SirReal2 (Tocris #5457). U2OS cells were also treated with DMSO (Millipore Sigma #D2660) alone as a control. After 24 hours of treatment, cells were harvested for protein or RNA extractions.

RNA-Seq Analysis of U2OS cells treated with Doxorubicin

For RNA-seq, U2OS cells were plated at 250,000 cells per well in a 6 well plate. The following day, cells were treated with either DMSO or 0.5μM Doxorubicin (n=3 per treatment). After 24 hour treatment, U2OS cells were washed with PBS and RNA was processed using a miRNeasy Mini Kit (QIAGEN) according to the protocol. The RNA concentration was quantified using NanoDrop Spectrophotometer (NanoDrop Technologies) and the integrity was validated by the OD260/OD280 absorption ration (>1.8). Samples were sequenced at Novartis Institute of Biomedical Research (Cambridge, MA) using Illumina HiSeq 4000 with alignment performed using EQP v2.3 and the NIBR Genome Reference system.

Read pairs were mapped to the Homo sapiens genome (GRCh38) and custom human genome, gene transcripts, and exon-exon junction fasta files derived from Ensembl (v76) using Exon-Quantification Pipeline (EQP) version 2.3. Average of

97.84% of total reads mapped to genome, transcript, or exon-exon junctions with 88.84% mapping to expressed reads. Aligned reads were used to calculate counts for gene, exon, and junctions based on Ensembl gene IDs (v90). Counts were converted to Transcripts Per kilobase Million (TPM) for downstream analysis. Differential expression analysis was performed on TPM values in R using edgeR and limma packages. Differential expression analysis for each contrast were calcualted using empirical Bayes moderate-t p-values with a minimum fold change of log2(2). Top adjusted p-values (Benjamini-Hochberg method adjusted for the number of genes per contrast) were extracted. Gene-set enrichment with Gene Ontology (GO) terms was performed using limma goana. GO terms were collected from GO.db R package (version 3.7.0).

Western Blot Analysis of U2OS cells with NAD-Boosting Compounds

For protein extractions, treated U2OS cells were washed with PBS and lysed at 4°C in RIPA lysis buffer with Halt® Protease and Phosphatase inhibitor cocktail (Thermo Fisher Scientific). Following a 30-minute incubation at 4°C, protein lysates were microcentrifuged in 1.5mL Eppendorf® tubes and the supernatants were collected for protein analysis. Protein concentrations were determined by a bicinchoninic acid (BCA) protein assay (Thermo Fisher Scientific, MA). Diluted proteins were separated by SDS-PAGE using a 4-20% Criterion TGX Precast Midi Protein Gel (Bio-Rad) and transferred to a nitrocellulose membrane by use of a Trans Turbo Blot system (Bio-Rad). Membranes were blocked with 5% milk in Tris-buffered saline with Tween-20® (TBS-T) for 1 hour at room temperature and were incubated with primary antibodies overnight at

4°C. The following day, membranes were washed three times with TBS-T and incubated with the appropriate HRP-conjugated secondary antibodies (Cell Signaling) for 1 hour at room temperature. The following primary antibodies were used at 1:1000 dilution: GAPDH (Cell Signaling #2118S), Acetyl-P53 (K382) (Cell Signaling #2525S), Total P53 (Calbiochem #OP43L), γH2AX (Thermo #MA1-2022), and Total H2AX (CST #7631S). The following secondary antibodies (Thermo Fisher Scientific) were used at 1:5000 dilution: Goat anti-Mouse IgG (H+L) Secondary Antibody, HRP (#31430) and Goat anti-Rabbit (H+L) Secondary Antibody, HRP (#31460).

RT-qPCR Analysis of U2OS cells with NAD-Boosting Compounds

Treated U2OS cells were washed with PBS and RNA was processed using a miRNeasy Mini Kit (QIAGEN) according to the protocol. Total RNA concentrations and quality were quantified using a NanoDrop™ spectrophotometer (NanoDrop™ Technologies, DE). cDNA was synthesized using 500ng total RNA by use of iScript™ cDNA synthesis kit (Bio-Rad). Once cDNA was synthesized, samples were diluted 1:10 in Ultra Pure distilled RNase-free water (Thermo Fisher Scientific). TaqMan® Fast Advanced Master Mix (Thermo Fisher Scientific) was used for all RT-qPCR assays in a 384-well optical plate format. Reactions were performed using a ViiA 7 RT-qPCR system (Thermo Fisher Scientific) and data analyzed by the threshold cycle ($\Delta\Delta CC_T$) method. The following human TaqMan® probes (Thermo Fisher Scientific) were used: Cdkn1a (Hs00355782_m1), Cdkn2a (HS00923894_m1), IL6 (HS00174121_m1), IL10 (Hs00961622_m1), IL1b (Hs01555410_m1), Gadd45a (Hs00169255_m1), Myc

(Hs00153408_m1), PUMA (Hs00248075_m1), TIGAR (Hs00608644_m1), SIRT1 (Hs01009006_m1), SIRT2 (Hs01560289_m1), NMRK1 (Hs00944470_m1), NMRK2 (HS01043681_m1), NAMPT (Hs00237184_m1), GDF15 (Hs00171132_m1), Col10a1 (Hs00166657_m1), NODAL (Hs00415443_m1), and Col6A5 (Hs00977391). All probes were multiplexed with GAPDH (Hs02786624_g1) as a housekeeping gene.

Statistics

Statistical significance was determined using GraphPad Prism 7.04 software by an unpaired Student's *t* test. All data are presented as a mean with standard error.

Chapter III

Results

DNA Damage and the NAD salvage pathway *in vivo*

The first goal of our study was to determine whether we could detect increased DNA damage in the tissues of aged animals. We were able to observe changes in post-translational modifications on PARP and P53 as readouts for the activity of DNA repair enzymes (Figure 3). PAR is a readout for the activity of PARP proteins, which are a family of enzymes in the nucleus that detect single stranded DNA breaks (Neuhaus et. al. 2015). Once PARP detects these breaks, it utilizes NAD to modify itself by the addition of poly-ADP ribose (PAR) chains. This modification acts as a signal to recruit other members of the DNA repair machinery to sites of DNA damage (D'Amours et al. 1999; Krishnakumar and Kraus 2010). Acetyl-P53 (K382) is a readout for both sirtuin activity and the upregulation of the P53 pathway. Normally P53 is degraded in the cell by the ubiquitin ligase MDM2. Upon various forms of cellular stress, like DNA damage, P53 becomes phosphorylated and acetylated at specific residues to block MDM2 binding and stabilize the protein (Schwartz and Rotter 1998). Stabilization of P53 stimulates transcription of downstream targets and halts the cell cycle in order for damaged DNA to be repaired. SIRT1 and SIRT2 are known to deacetylate Acetyl-P53 (K382) in order to regulate P53 activity (Kouzarides et. al. 2002). We were able to observe a significant increase in PAR and Acetyl-P53 (K382) in 27-month old mouse kidneys compared to 6-month old mice. This detectable increase in DNA damage with age aligns with

publications suggesting that the chronic activation of PARP leads to an impairment in sirtuin activity due to changes in NAD and NAM levels. Total PARP and GAPDH levels were not significantly different between young and aged animals.

In order to link the imbalance of DNA repair enzymatic activity to the reported decline in NAD levels with age, we measured changes in metabolites associated with the NAD salvage pathway (Figure 2). Levels of NAD, NADH, and SAM were significantly lower in both cohorts of aged animals (Figure 4). While NAM and NMN levels remained unchanged between young and aged animals, 1-Me-NAM was significantly upregulated in aged animals in Cohort 2. These results confirm the association of increased DNA damage in aged animals with the dysregulation of metabolites within the NAD salvage pathway.

DNA damage-induced *in vitro* model of Disease Progression

Next, we wanted to develop a DNA damage-induced *in vitro* model to determine whether we could mimic the increase of DNA damage markers that we observed in aged animals. Following in the footsteps of the McKnight lab who discovered P7C3, a small molecule that activates NAMPT, we dosed U2OS cells with sub lethal doses of Doxorubicin to initiate DNA damage. We then profiled these cells by RNA-seq and identified pathways associated with DNA damage and senescence (Figure 5). Genes associated with cell cycle arrest and DNA repair such as Cdkn1a, DDB2, RAD51C, BTG2, FAS, and SUSD8 were significantly upregulated with Doxorubicin treatment compared to DMSO treated control cells (Broustas and Lieberman 2014; Wood et al.

2001). A number of genes associated with the upregulation of the P53 pathway were expressed including Gadd45a, Bbc3, MDM2, Gpr87, TIGAR, SES1, SES2, TP53, and RR2B (Fisher 2017). We then decided to search for genes associated with a SASP or pro-inflammatory response and confirmed the upregulation of EPN3, STAT4, RELB, TNFAIP3, SULF2, CYP4F3, IL7R, TLR3, ICAM1, CCL4, TRAF1, IGFBP2, and BCL2A1 as a result of Dox-induced DNA damage (Coppe et al. 2010) (Figure 6). Finally, and perhaps more remarkably, we observed a significant upregulation of genes associated with fibrosis. A number of these genes were related to collagen production including COL17A1, COL27A1, COL6A5, COL19A1, COL10A1, COL25A1, COL9A1, COL7A1, COLCA1, and COL20A1 (Wei et al. 2017; Cox et al. 2013; Egebald et al. 2010). Likewise, some well-known fibrosis markers were upregulated in this model including GDF15, ACTA2, TSPAN11, TGFA, NODAL, Serpine1, and TMEM173 (Zhang et al. 2019; Alsafadi et al. 2017; Biernacka et al. 2011; Qiu et al. 2017). This transcriptional cascade effect in our cellular model gave us confidence that this system could not only mimic an age-associated increase in DNA damage markers, but also give us insight into whether published compounds reported to improve DNA repair capacity could counter regulate many of these age-associated genes.

Benefits of NAD-boosting therapies on SIRT activity and DNA repair capacity

Next, we wanted to directly compare the benefits of NR supplementation to the activation of NAMPT by P7C3 administration in our cellular DNA damage model. As previously described, the conversion of NR to NMN in the cell is initiated by the

phosphorylation of NR by NRK1 and NRK2 (Ratajczack et al. 2016). In order to confirm that Nicotinamide Riboside could be utilized by U2OS cells, NRK1 and NRK2 transcription levels were measured by RT-qPCR. NRK1, NRK2, and NAMPT transcription levels were expressed in U2OS cells and were not significantly altered by Doxorubicin treatment compared to DMSO treated cells (Figure 8).

Since we knew that Doxorubicin treatment increased markers associated with cell cycle arrest, we wanted to determine whether cotreatment with these compounds could improve cell viability. We coadministered U2OS cells with Doxorubicin and either NR or P7C3 in 16-point dose response for 72 hours using Cell Titer Glo® as our readout for cell viability. Nicotinamide Riboside did not significantly improve ATP or cell viability whereas P7C3 increased cell viability at doses that ranged between 0.2 and 25μM (Figure 9). We hypothesize that P7C3 demonstrates a bell-shaped curve for cell viability as it may exhibit toxicity at 50μM.

Benefits of NAD-boosting therapies on transcriptional markers associated with DNA-damage induced Disease Progression

Next, we wanted to determine whether NR or P7C3 could improve sirtuin activity or increase DNA repair capacity in our DNA damage model. We cotreated U2OS cells with Doxorubicin and either NR or P7C3 for 24 hours (Figure 10). We then detected and quantified levels of Acetyl-P53 (K382) as a readout for sirtuin activity and γH2AX as a readout for double stranded DNA breaks. All three doses of P7C3 demonstrated a

modest decrease in acetylation of P53 (K382), total P53, γH2AX (Ser139), and total H2AX suggesting activation of the sirtuins and an improvement in DNA repair capacity. On the other hand, NR treatment seemed to have no beneficial effect SIRT activity and exhibited a modest decrease in γH2AX and Total H2AX levels at 500μM.

In order to confirm that the benefits of P7C3 on Acetyl-P53 (K382) were driven by the activation of the sirtuins, we treated U2OS cells in our DNA damage assay with Doxorubicin, P7C3 and either a SIRT1 (Ex527) or SIRT2 inhibitor (SirReal2) (Figure 11). We confirmed that P7C3 treatment leads to a modest reduction in Acetyl-P53(K382). Administration of a SIRT1 inhibitor increased the acetylation of P53 (K382) two-fold; however, P7C3 was still able to modulate Acetyl-P53 (K382) when cotreated with a SIRT1 inhibitor. On the other hand, coadministration of a SIRT2 inhibitor and P7C3 blocked the P7C3-associated decrease in Acetyl-P53 (K382), suggesting that P7C3 may increase NAD levels and act on P53 through SIRT2 activation.

Finally, we wanted to determine whether P7C3 or NR administration could counter regulate genes associated with DNA damage, senescence, inflammation and fibrosis that we identified from our RNA-seq data analysis. Cdkn1a (p21) and Cdkn2a (p16) are common markers associated with cell cycle arrest and replicative senescence, respectively (Collado and Serrano 2010). NR increased levels of p21 and had a modest effect on p16 levels at 500μM treatment (Figure 12). P7C3 had no effect on p21, but significantly downregulated expression of p16. Next, we chose to examine expression levels of Gadd45a, PUMA, TIGAR and Myc, which are DNA damage markers downstream of the P53 pathway (Green and Chipuk 2006) (Figure 12). P7C3 counter regulated all of these markers associated with P53 activation whereas NR administration

exhibited no detectable changes. While P7C3 exhibited a modest change in Acetyl-P53 (K382) levels, this change resulted in significant downregulation of genes associated with senescence and the P53 pathway. These results correlate with our Cell Titer Glo® assay where P7C3 was able increase ATP levels and improve cell viability.

Next, we assessed the expression of markers associated with a pro-inflammatory response (Figure 13). Both NR and P7C3 increased IL6 transcription; however, P7C3 significantly reduced levels of IL10 and IL1b in a dose-dependent manner. Finally, we examined the expression levels of GDF15, Col10a1, NODAL, and Col6a5 as markers associated with fibrosis (Figure 14). P7C3 counter regulated transcription levels of GDF15, Col10a1, and NODAL. NR had no effect of GDF15, Col10a1, or Col6a5, but significantly reduced transcription levels of NODAL at 500μM. Through this dataset, we observed that NAMPT activation by P7C3 was superior to NR supplementation regarding the counter regulation of genes associated with DNA damage, senescence, inflammation and fibrosis.

In addition to looking at these DNA damage-related transcriptional changes, we measured the expression levels of SIRT1, SIRT2, NAMPT, NRK1, and NRK2 in order to determine whether NR and P7C3 modulated expression of these enzymes (Figure 15). Relative expression levels of SIRT1 and NAMPT did not change with administration of NR or P7C3. However, both NR and P7C3 significantly upregulated SIRT2 and NRK1 transcription levels. While there are no publications confirming that NR and P7C3 modulate these genes, we hypothesize that NRK1 transcription may increase as a result of increased levels of NR to be utilized by the cell. However, it is unclear why NR would upregulate SIRT2 expression considering NR did not deacetylate Acetyl-P53 (K382). On

the other hand, perhaps P7C3 increases SIRT2 expression as a consequence of increasing SIRT2 activity; however, there are no published reports demonstrating that increased Sirt2 activity affects Sirt2 transcription or data suggesting that P53 modulation directly affects SIRT2 transcription. Future work should be done to determine why P7C3 would increase NRK1 and SIRT2 transcription.

Chapter IV

Discussion

Significance of Results

DNA damage accumulation has been linked to an age-related decline in NAD levels leading to the progression of many age-related pathologies (Gomes et. al. 2013; Zhu et. al. 2015; Zhang et. al. 2016). We were able to observe an upregulation of PARP activity and inhibition of the sirtuins through the P53 pathway in the kidneys of aged mice (Figure 3). As previously mentioned, in states of increased or persistent DNA damage, PARP has a higher affinity for NAD causing it to be chronically upregulated (Mouchiroud et al. 2013; Gomes et al. 2013; Yoshino et al. 2013). As a result, chronic activation of PARP leads to a depletion of NAD and an increase in NAM, causing sirtuin inhibition and an impairment in DNA repair capacity. We were able to capture a significant reduction in NAD and NADH metabolite levels in aged mouse kidneys compared to their young counterparts (Figure 4). Interestingly, while NAM levels did not change between young and aged animals, one animal cohort exhibited a significant increase in 1-Me-NAM. We hypothesize that this difference between animal cohorts as well as the overall differences in metabolite levels is indicative of the natural variability within aging. These results are in line with publications demonstrating that small changes in these metabolites can have profound impacts on cellular processes that rely on the NAD salvage pathway (Gomes et. al. 2013; Zhu et. al. 2015; Zhang et. al. 2016). The observed increase in 1-Me-NAM along with a reduction in the universal methyl donor,

SAM, suggests that elevated levels of NAM levels may be captured through the increase of 1-Me-NAM as a means to export excess NAM out of the cell (Figure 2). This observed decrease in NAD and increase in 1-Me-NAM may explain why we can detect increased levels of PARP activity at the same time that we can detect decreased levels of sirtuin activity.

Following these observations in aged animals, we were able to generate a DNA damage *in vitro* model by dosing U2OS cells with sub lethal doses of Doxorubicin. Not only were we able to detect an increase in Acetyl-P53 (K382) and γH2AX levels with Dox-treatment (Figure 10), we were also able to capture the upregulation of genes associated with DNA damage, senescence, inflammation, and fibrosis (Figures 5-7). This model correlates with published literature surrounding the development of age-associated diseases as well as the occurrence of radiation-induced fibrosis observed in cancer patients (Serrano et. al. 2014; Straub et. al. 2016).

Using this cellular system for DNA damage, we were able to directly compare the mechanisms of NR supplementation to NAMPT activation through P7C3 administration. P7C3 was able to improve cell viability, increase sirtuin activity, and improve DNA repair capacity (Figure 9 and 10). We then confirmed that the benefits of NAMPT activation on sirtuin activity could be blocked by cotreatment with a SIRT2 inhibitor suggesting that P7C3 can increase NAD levels and activate SIRT2 (Figure 11). These modest changes in sirtuin activity with P7C3 administration resulted in the significant counter regulation of genes associated with increased senescence, P53 upregulation, pro-inflammatory response, and fibrosis (Figures 12-14). On the other hand, while NR supplementation exhibited a modest decline in γH2AX levels, Total H2AX and p16

expression at high doses, NAMPT activation with P7C3 was superior to NR supplementation to improve DNA repair capacity in a model of increased DNA damage.

Study Limitations

One major research limitation of this study is whether our Doxorubicin-induced DNA damage system can be reflective of what is happening in an aged system. Typically, DNA damage causes impaired cells to become senescent, resulting in the recruitment of immune cells that try to clear away the senescent cells and regenerate the tissue. This SASP response becomes dysregulated with aging leading to fibrosis and tissue dysfunction. This crosstalk between multiple cell types is very difficult to recreate in an *in vitro* setting; therefore, future work would be needed to compare the observed cascade effect of our DNA damage model to a time course model of aging or a particular disease state.

Another limitation of this study is whether our DNA damage assay exhibits the same effects on metabolites in the NAD salvage pathway as we observed in aged animals. In the future, we should determine whether Doxorubicin treatment alters NAD, NAM, and other metabolites relevant to sirtuin activation and DNA repair capacity. Once that work is completed, it would be beneficial to compare how P7C3 and NR administration modulate these metabolites directly.

Finally, it is unclear from our results whether the benefits of P7C3 increase NAD or increase SIRT2 transcription levels. Based on our data, we know that a SIRT2

inhibitor blocks the benefits of P7C3 on Acetyl-P53 (K382) and treatment with P7C3 increases SIRT2 transcription (Figures 11 and 15). One hypothesis suggests that P7C3 could directly increase SIRT2 transcription and therefore improve its activity. Alternatively, P7C3 could increase NAD pools in the cytoplasm, leading to the activation of SIRT2 and an increase in its transcription levels. While the McKnight lab was able to demonstration that NAMPT is the target of P7C3, we hope future work will confirm this mechanism in our assays.

Future Research Directions

Research building on these results should focus on why the mechanism of P7C3 is superior to NR administration at improving cell proliferation, sirtuin activation, and DNA repair capacity in the context of increased DNA damage levels. While NR treatment directly increases levels of NAD, P7C3 is a small molecule that activates NAMPT to convert NAM to NMN. In our *in vitro* model for DNA damage, NR administration does not seem to improve cell proliferation, activate the sirtuins, or enhance DNA repair capacity. However, the mechanism of P7C3 to utilize and recycle NAM pools back through the NAD salvage pathway seems to have beneficial effects on not only SIRT activity and DNA repair capacity, but also to counter regulate genes associated with senescence, inflammation and fibrosis. DNA damage leads to increased activation of DNA repair enzymes, causing a depletion of NAD and an increase in NAM. As we observed in aged animals, the increase in 1-Me-NAM suggests a need to export increased levels of NAM out of the cell due to the chronic upregulation of PARP (Pissios 2017).

Many publications surrounding NR supplementation discuss the benefits of boosting NAD and use increased levels of NAM as a beneficial marker for the upregulation of DNA repair enzymes. However, it is clear from our results that NR administration may actually impair sirtuin activity and DNA repair capacity.

Conclusion

I hypothesized that both Nicotinamide Riboside and P7C3 would have beneficial effects on sirtuin activation, DNA repair capacity, and markers associated with disease progression in the context of high DNA damage. It is clear from our results that P7C3 was superior to NR to activate the sirtuins and improve DNA repair capacity. The results of the study suggests that there may be consequences to administer NR in the context of high levels in DNA damage, particularly in age-related indications where increasing NAM levels may effect sirtuin activity and DNA damage response.

Appendix

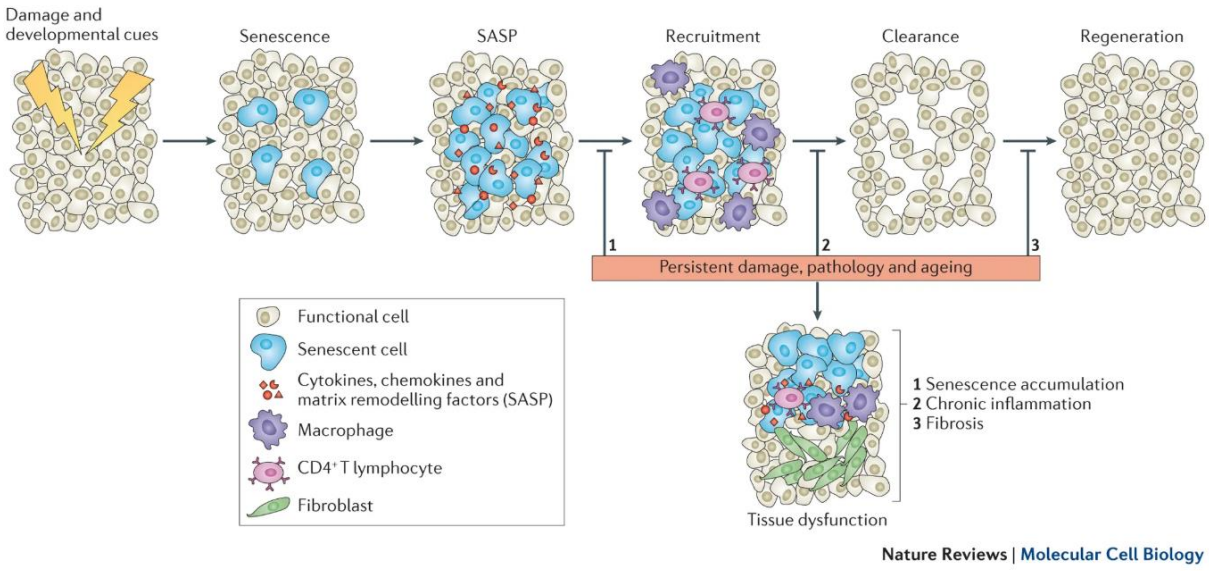

Figure 1. Mechanism by which tissue regeneration becomes dysregulated with persistent damage, age, and pathology as a result of increased DNA damage (Munoz-Espin and Serrano, 2014).

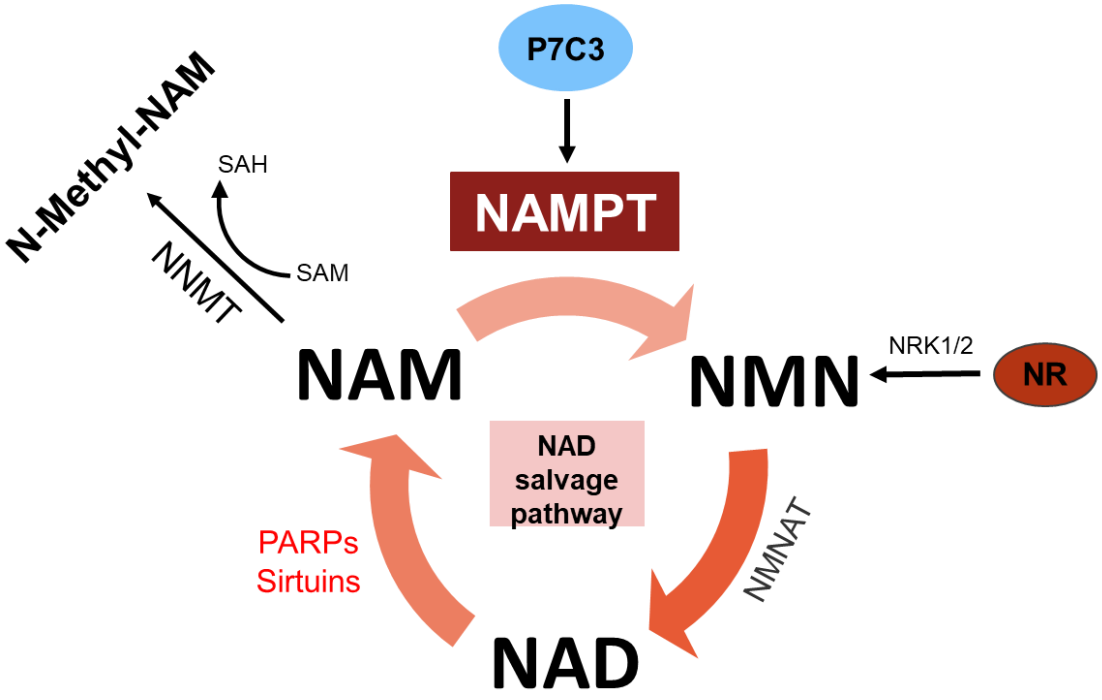

Figure 2: Mechanistic figure of the nicotinamide adenine dinucleotide (NAD) salvage pathway. Typically, NAD is generated through the NAD salvage pathway. NAD is consumed by the sirtuins and PARPs, causing the release of Nicotinamide (NAM) as a byproduct. NAM is converted to Nicotinamide mononucleotide (NMN) by Nicotinamide phophoribosyltransferase (NAMPT), the rate-limiting step of the NAD salvage pathway. NMN is then subsequently converted to NAD by the enzymes Nicotinamide mononucleotide adenylyl transferases 1-2 (NMNAT 1-3). Excess levels of NAM that are not recycled through the salvage pathway are methylated by Nicotinamide N-methyltransferase (NNMT) using the universal methyl donor S-Adenosyl methionine (SAM) to produce S-adenosyl-L-homocysteine (SAH) and N-Methyl-NAM to be exported out of the cell. P7C3 is a reported activator of NAMPT that can utilize excess levels of NAM and recycle NAM back through the salvage pathway to generate NMN. Nicotinamide Riboside (NR) offers an alternative to enzyme activation where NRK1/2 phosphorylate NR to NMN which is then converted to NAD by NMNAT1-3 (Pissios 2017).

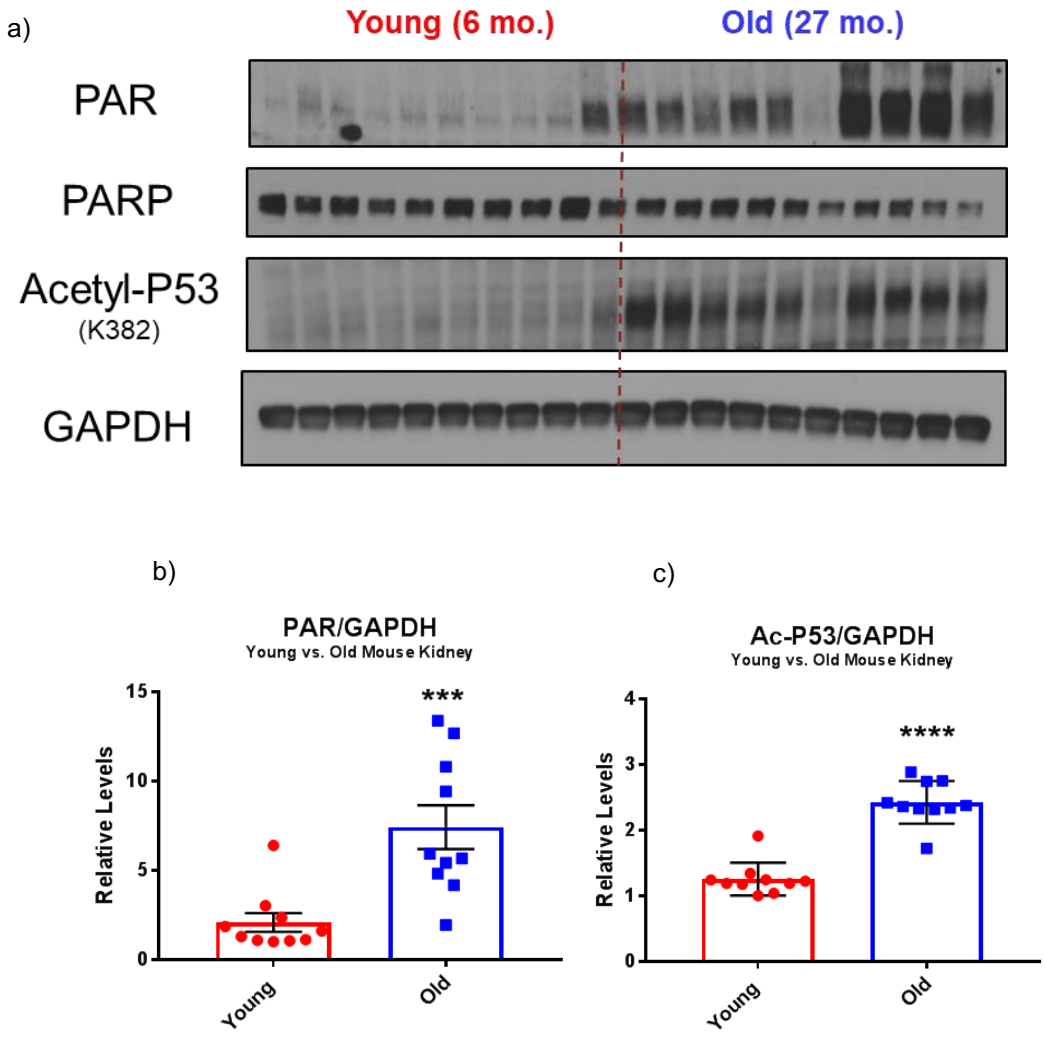

Figure 3. The dysregulation of DNA repair enzymes is detectable in aged mouse kidney. a) Representative immunoblots are shown for PAR, PARP, and Acetyl-P53 (K392) in the kidneys of 6- and 27-month of mice (n=8 per group). Glyceraldehyde-3-phosphate dehydrogenase (GAPDH) is shown as a protein loading control. Levels of b) PAR and c) Acetyl-P53 relative to GAPDH were quantified by densitometry. Data are mean ± standard error of the mean. Statistical significance was determined by unpaired Student's *t* test. Asterisks are used to denote significance as follows: ***, $P < 0.001$; ****, $P < 0.0001$.

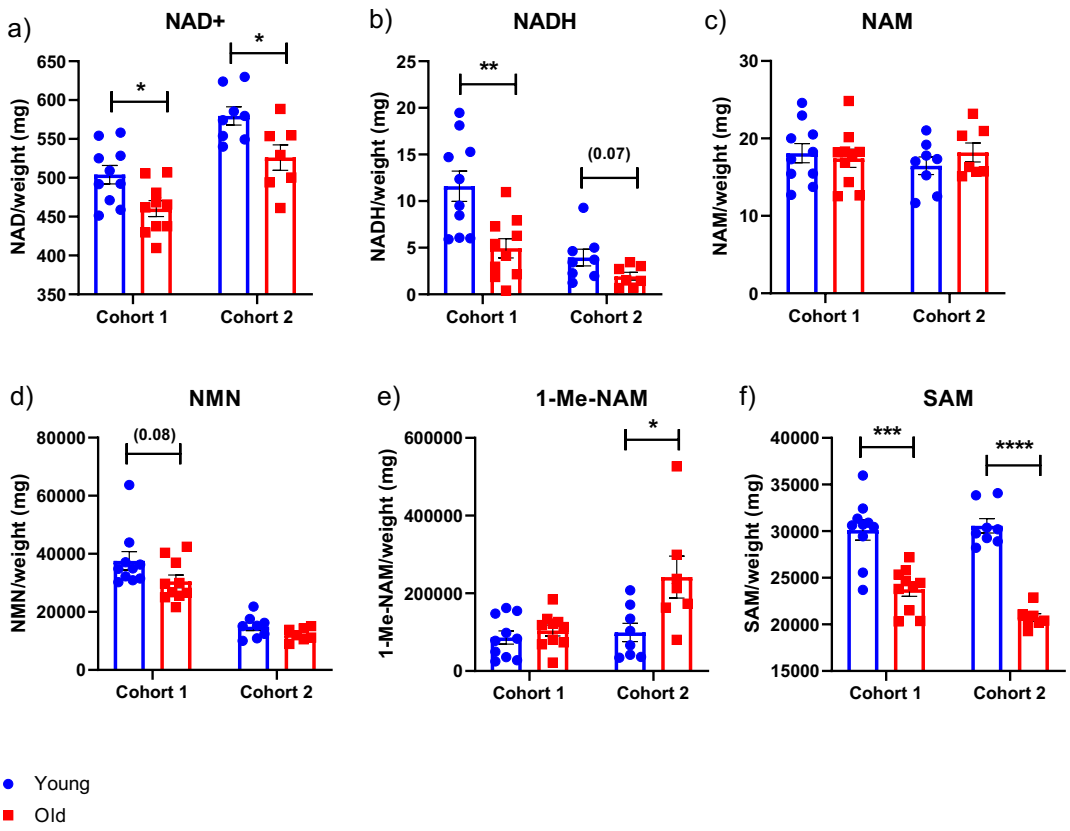

Figure 4. Metabolites within the NAD salvage pathway are dysregulated in aged mice compared to young mice. Data is shown normalized to tissue weight for the following metabolites: (a) NAD+, (b) NADH, (c) NAM, (d) NMN, (e) 1-Me-NAM, and (f) SAM. The following dataset compared metabolite levels in two animal cohorts. Cohort 1 compares metabolite levels in the kidneys of 6- and 27-month of C57Bl6/N mice (n=8 per group). Cohort 2 compares metabolite levels in the kidneys of 6- and 24- month old C57Bl6/J mice (n= 8 and 7, respectively). Data are mean ± standard error of the mean. Statistical significance was determined by unpaired Student's *t* test. Asterisks are used to denote significance as follows: *, $P < 0.05$, **, $P < 0.01$; ***, $P < 0.001$.

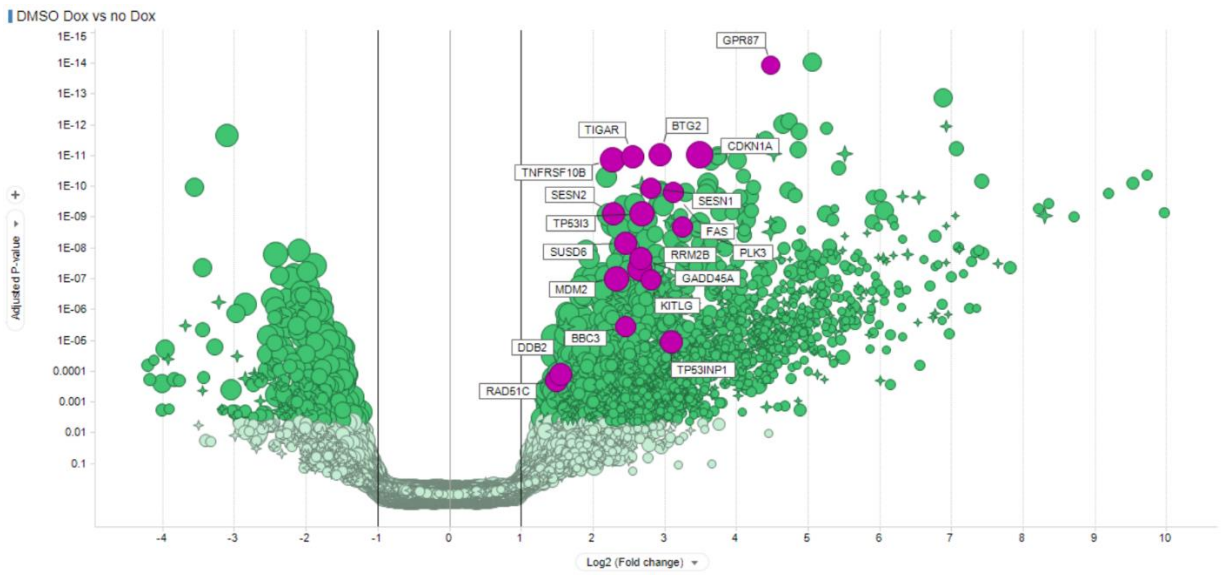

Figure 5. Transcriptional markers associated with DNA damage and senescence are upregulated in U2OS treated with Doxorubicin, a DNA damage-inducing agent. The y-axis represents the adjusted P-value. The x-axis represents the Log2 (Fold Change) comparing DMSO treated cells to 0.5µM Doxorubicin treated cells.

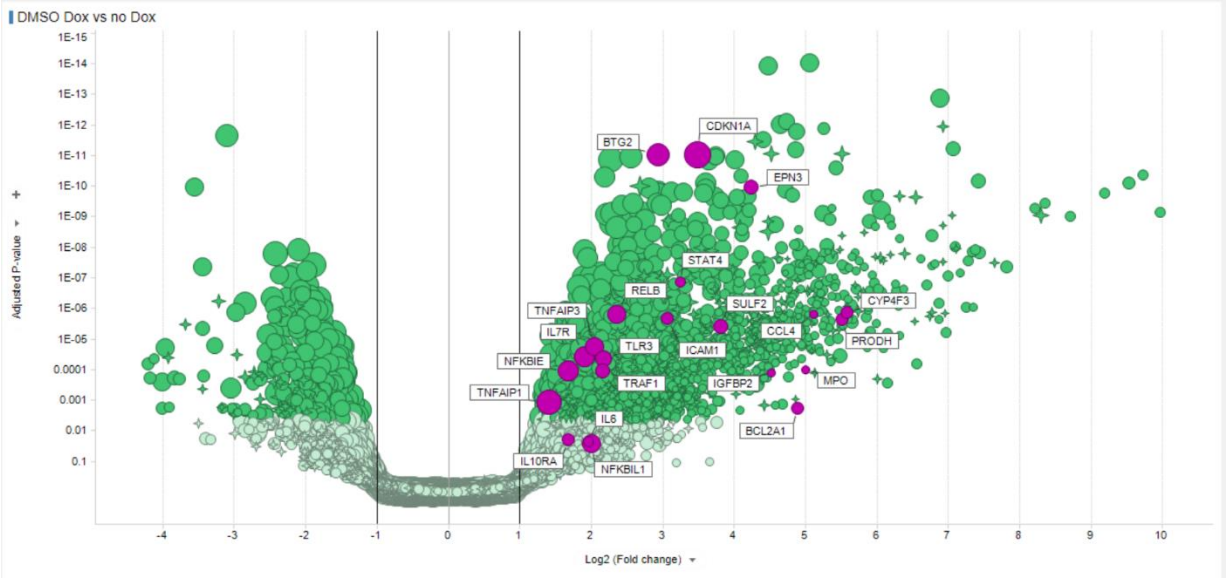

Figure 6. Transcriptional markers associated with the secretory associated senescence phenotype (SASP) response are upregulated in U2OS cells treated with Doxorubicin, a DNA-damage inducing agent. The y-axis represents the adjusted P-value. The x-axis represents the Log2 (Fold Change) comparing DMSO treated cells to 0.5µM Doxorubicin treated cells.

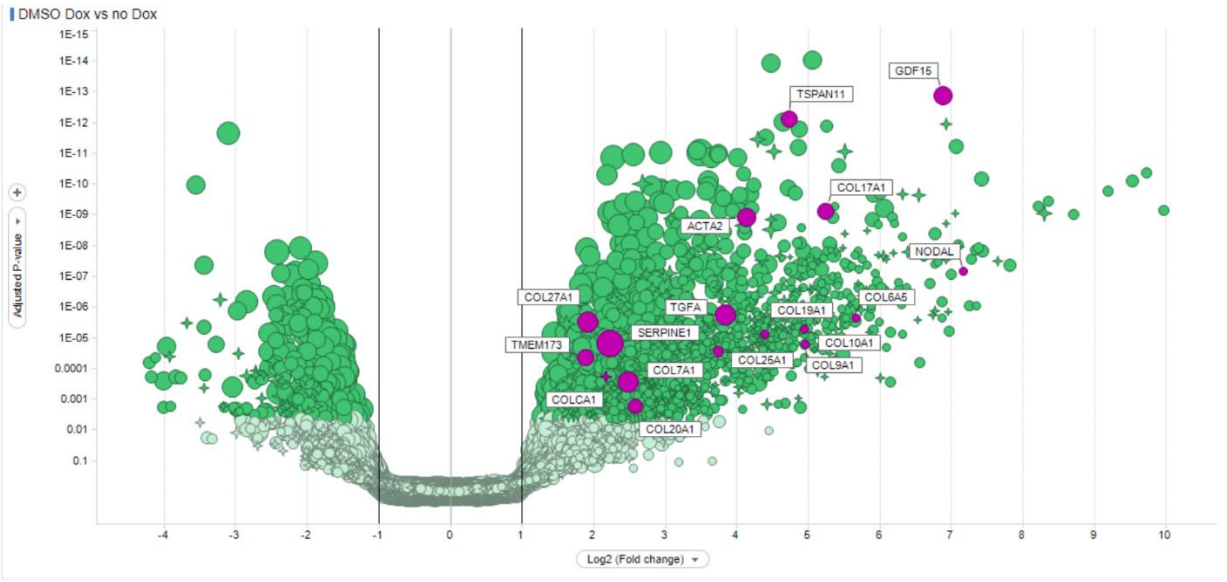

Figure 7. Transcriptional markers associated with fibrosis are upregulated in U2OS treated with Doxorubicin, a DNA-damage inducing agent. The y-axis represents the adjusted P-value. The x-axis represents the Log2 (Fold Change) comparing DMSO treated cells to 0.5µM Doxorubicin treated cells.

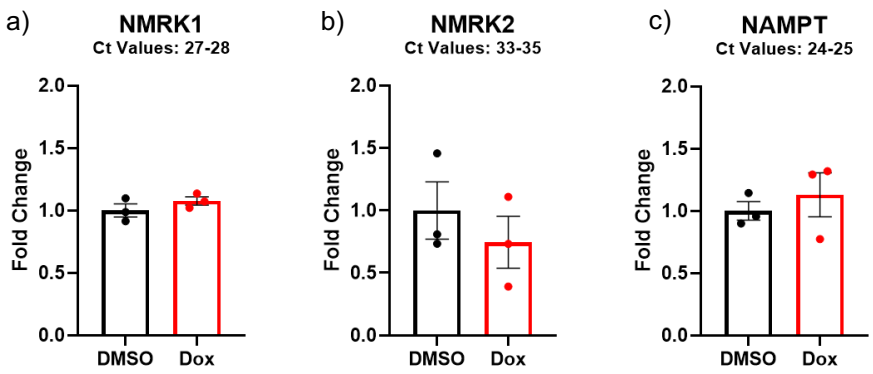

Figure 8. Transcription expression levels of a) NRK1, b) NRK2, and c) NAMPT are detectable in U2OS cells and do not change with Doxorubicin treatment. Data are mean ± standard error of the mean. Statistical significance was determined by unpaired Student's *t* test.

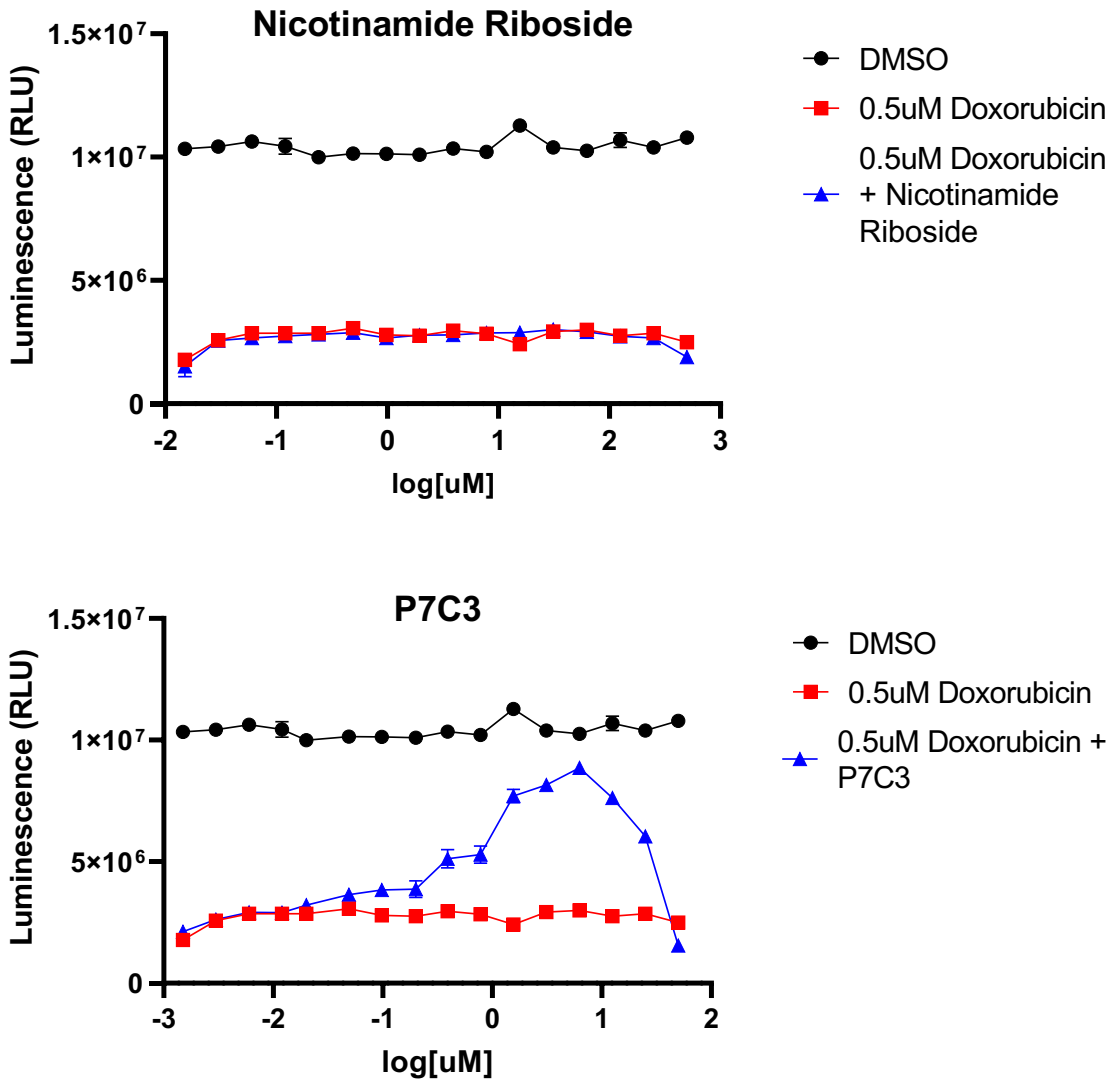

Figure 9. P7C3 increases cell viability in U2OS cells treated with Doxorubicin whereas Nicotinamide Riboside has not effect on cell viability. Data are mean ± standard error of the mean.

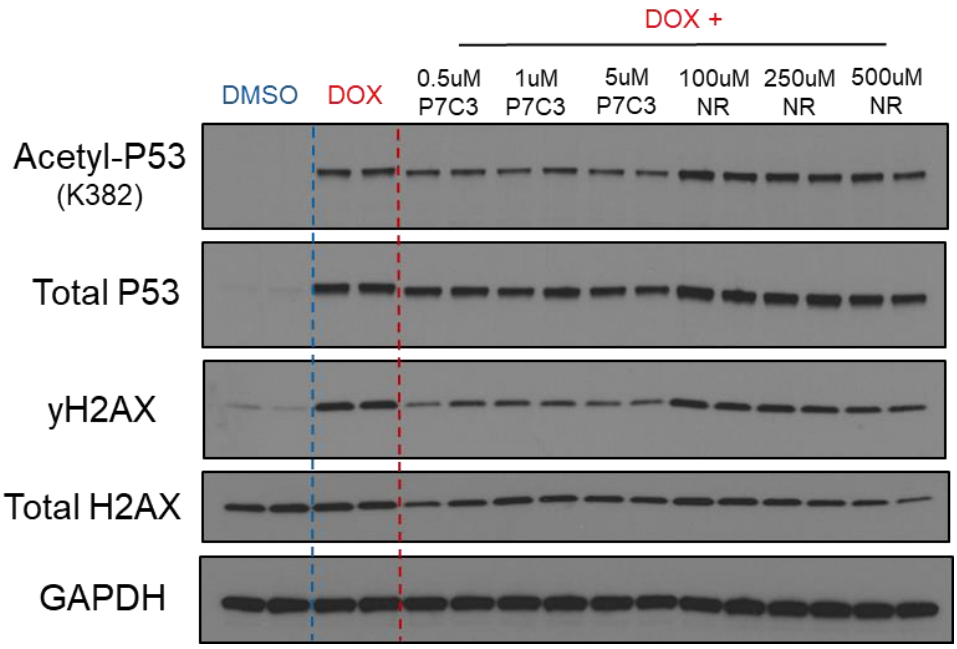

Figure 10. P7C3 treatment activates the sirtuins and improves DNA repair capacity in U2OS cells dosed with Doxorubicin. Representative immunoblots are shown for Acetyl-P53 (K392), Total P53, γH2AX, and Total H2AX in U2OS cells treated with 0.5μM Doxorubicin for 24h. Glyceraldehyde-3-phosphate dehydrogenase (GAPDH) is shown as a protein loading control.

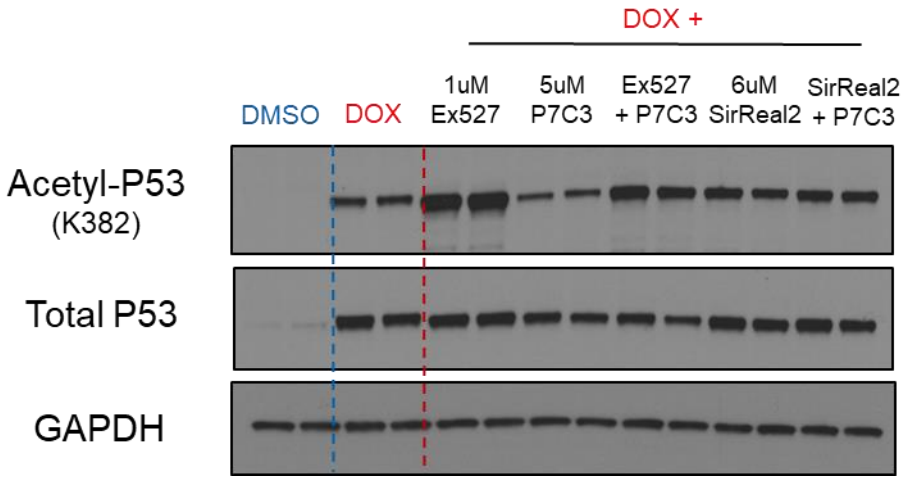

Figure 11. The benefits of P7C3 on sirtuin activation are blocked with the addition of Ex527, a SIRT1 inhibitor, and SirReal2, a SIRT2 inhibitor in U2OS cells dosed with Doxorubicin. Representative immunoblots are shown for Acetyl-P53 (K392) and Total P53 in U2OS cells treated with 0.5µM Doxorubicin for 24h. Glyceraldehyde-3-phosphate dehydrogenase (GAPDH) is shown as a protein loading control.

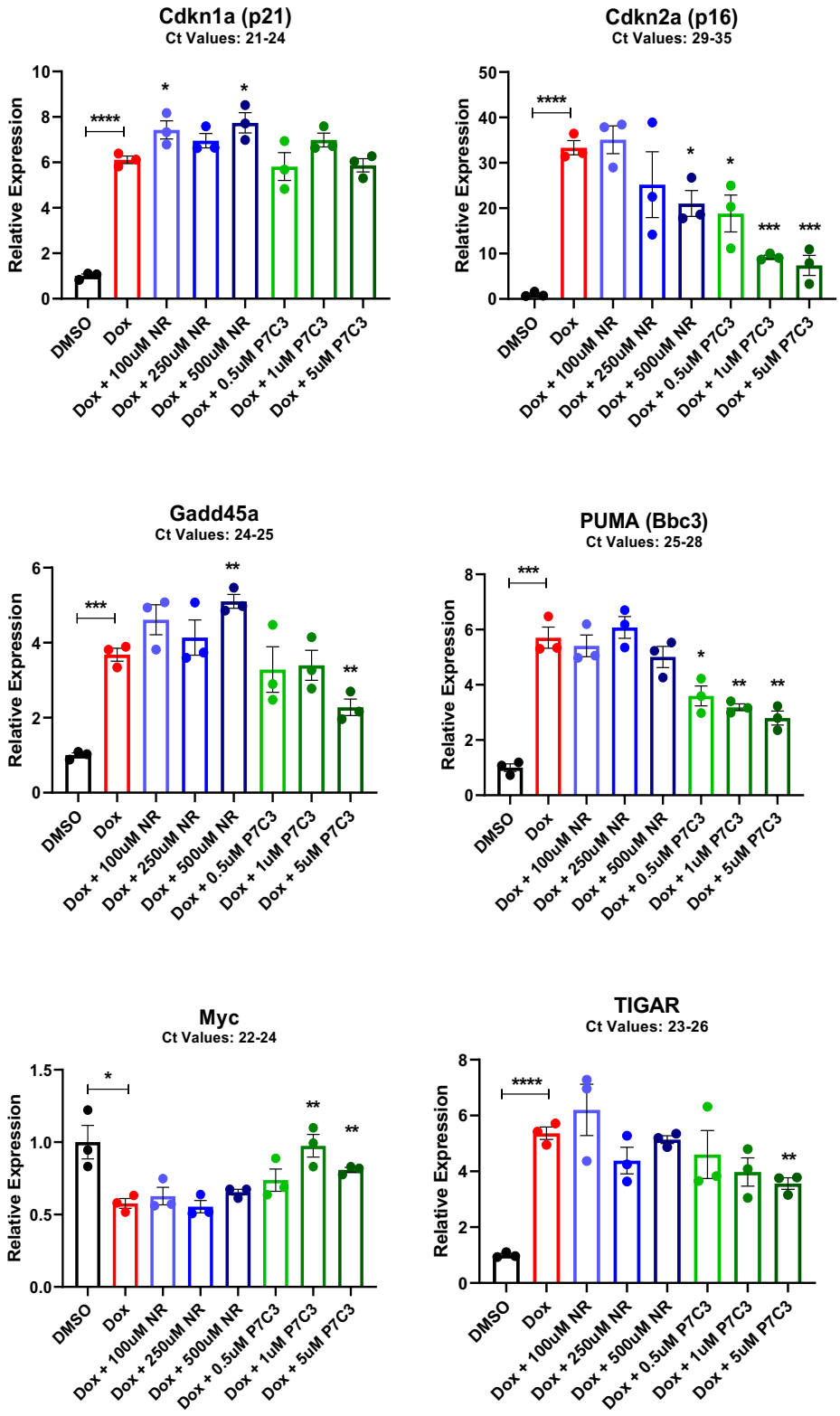

Figure 12. P7C3 counter regulates transcriptional markers associated with senescence and DNA damage in U2OS cells dosed with Doxorubicin. Data are mean ± standard error of

the mean. Statistical significance was determined by unpaired Student's *t* test. Asterisks are used to denote significance as follows: *, $P < 0.05$, **, $P < 0.01$; ***, $P < 0.001$, ***.

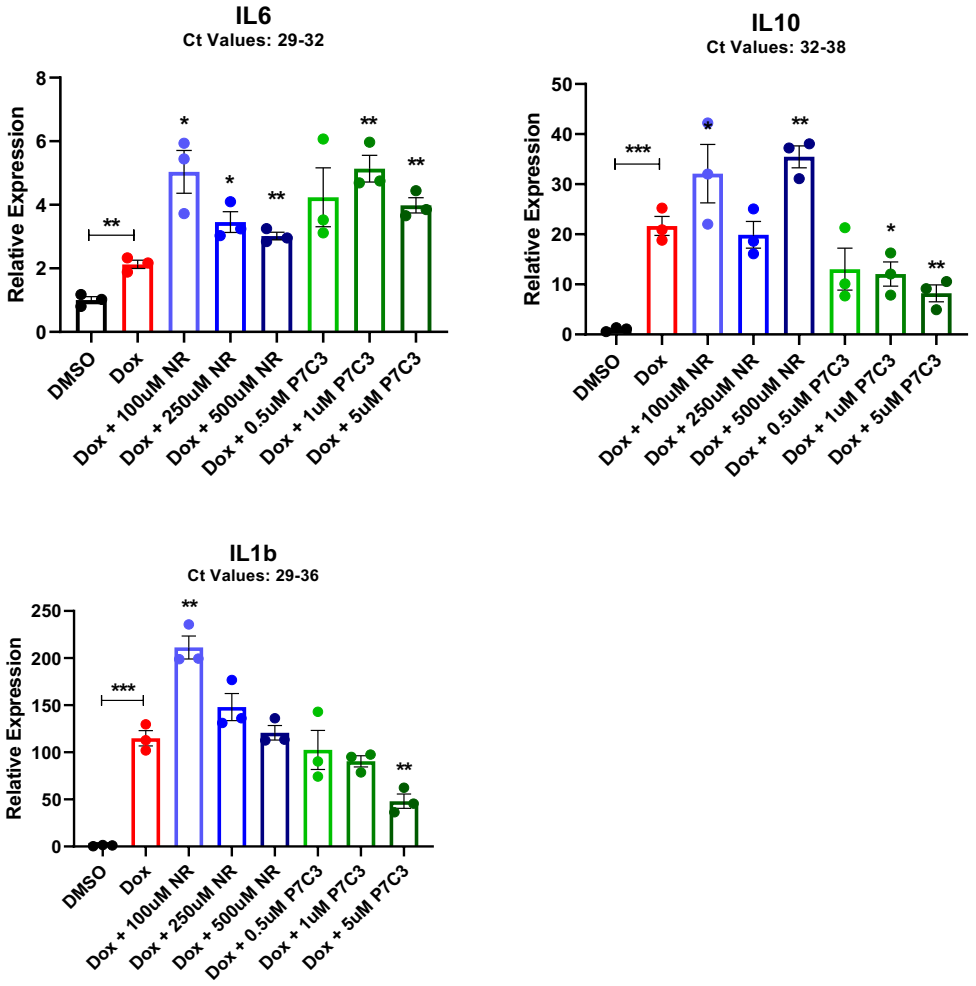

Figure 13. P7C3 counter regulates genes associated with inflammation in U2OS cells dosed with Doxorubicin. Data are mean ± standard error of the mean. Statistical significance was determined by unpaired Student's *t* test. Asterisks are used to denote significance as follows: *, $P < 0.05$, **, $P < 0.01$; ***.

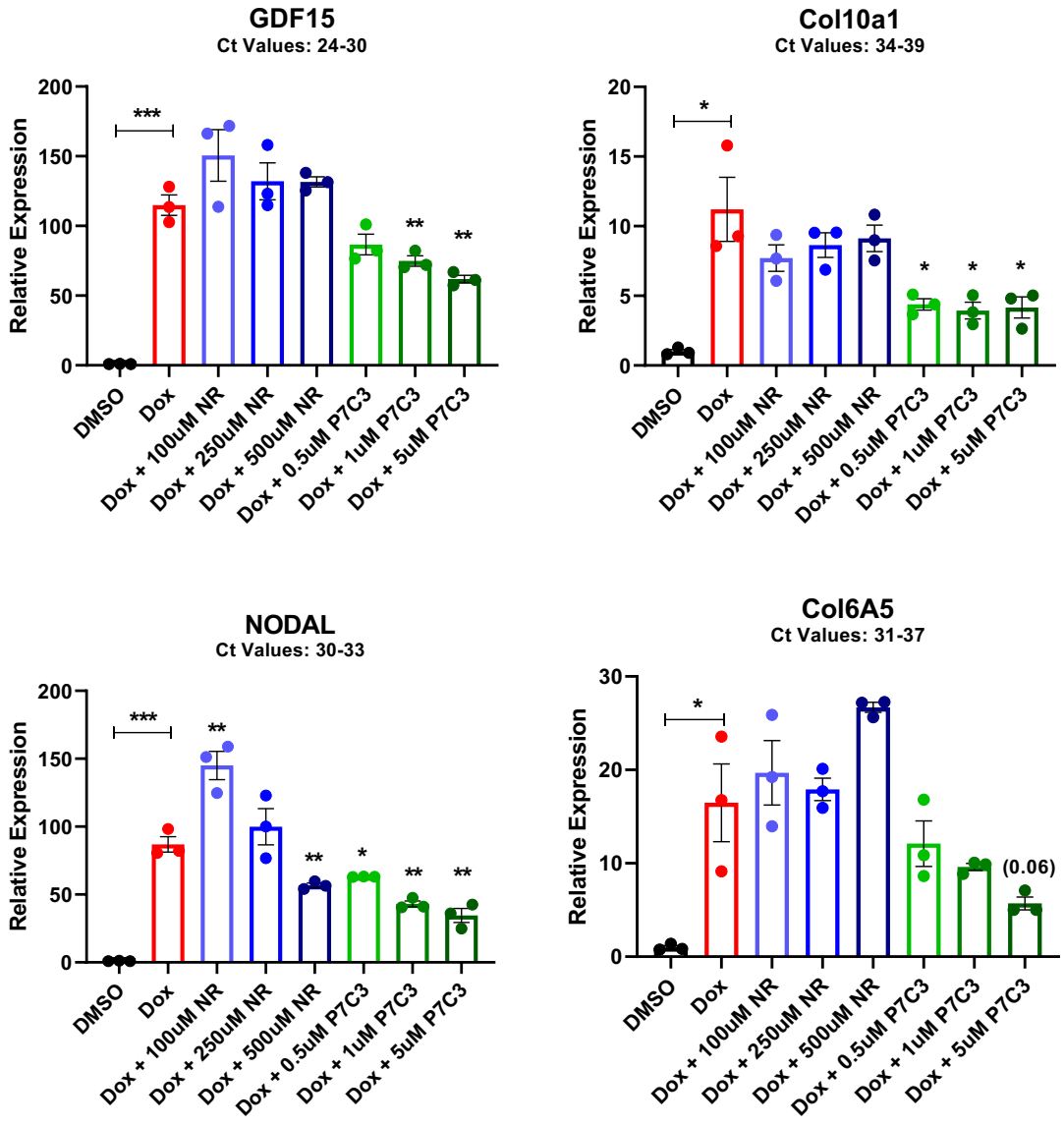

Figure 14. P7C3 counter regulates transcriptional markers associated with fibrosis in U2OS dosed with Doxorubicin. Data are mean ± standard error of the mean. Statistical significance was determined by unpaired Student's *t* test. Asterisks are used to denote significance as follows: *, $P < 0.05$, **, $P < 0.01$; ***, $P < 0.001$.

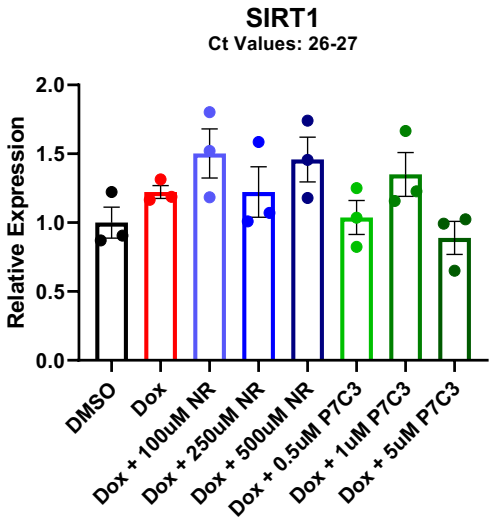
SIRT1
Ct Values: 26-27
Relative Expression
2.0
1.5
1.0
0.5
0.0
DMSO
Dox
Dox + 100uM NR
Dox + 250uM NR
Dox + 500uM NR
Dox + 0.5uM P7C3
Dox + 1uM P7C3
Dox + 5uM P7C3

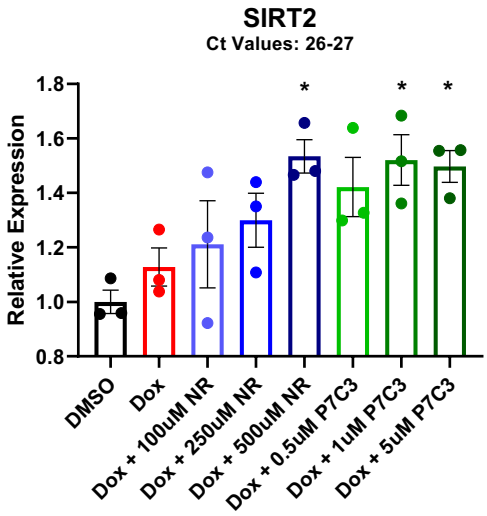
SIRT2
Ct Values: 26-27
Relative Expression
1.8
1.6
1.4
1.2
1.0
0.8
*
*
*
DMSO
Dox
Dox + 100uM NR
Dox + 250uM NR
Dox + 500uM NR
Dox + 0.5uM P7C3
Dox + 1uM P7C3
Dox + 5uM P7C3

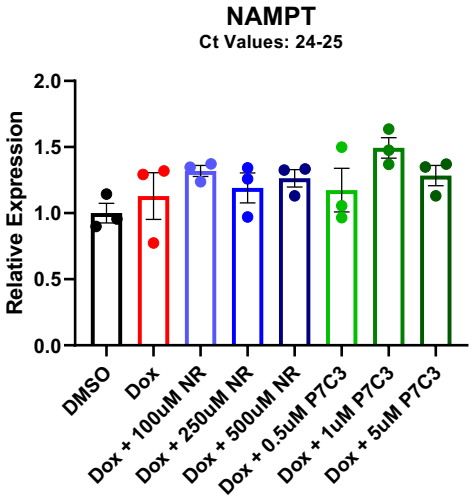
NAMPT
Ct Values: 24-25
Relative Expression
2.0
1.5
1.0
0.5
0.0
DMSO
Dox
Dox + 100uM NR
Dox + 250uM NR
Dox + 500uM NR
Dox + 0.5uM P7C3
Dox + 1uM P7C3
Dox + 5uM P7C3

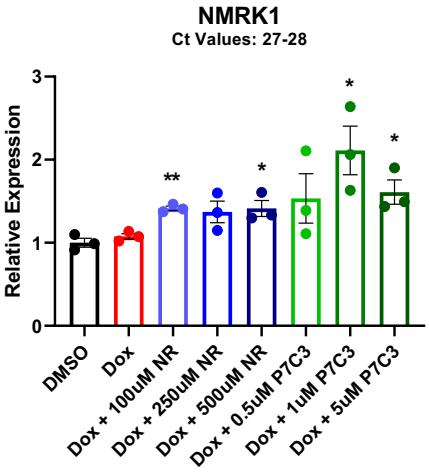
NMRK1
Ct Values: 27-28
Relative Expression
3
2
1
0
**
*
*
*
DMSO
Dox
Dox + 100uM NR
Dox + 250uM NR
Dox + 500uM NR
Dox + 0.5uM P7C3
Dox + 1uM P7C3
Dox + 5uM P7C3

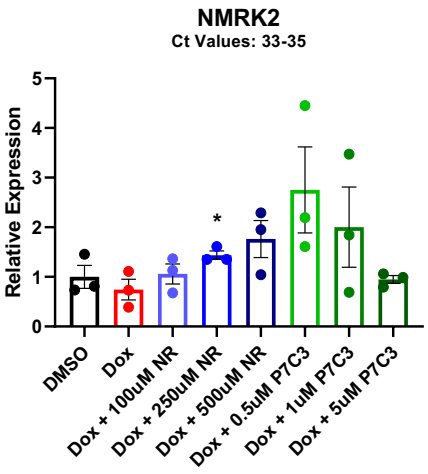
NMRK2
Ct Values: 33-35
Relative Expression
5
4
3
2
1
0
*
DMSO
Dox
Dox + 100uM NR
Dox + 250uM NR
Dox + 500uM NR
Dox + 0.5uM P7C3
Dox + 1uM P7C3
Dox + 5uM P7C3

Figure 15. NR and P7C3 increases SIRT2 and NMRK1 transcription levels in U2OS dosed with Doxorubicin. Data are mean ± standard error of the mean. Statistical significance was determined by unpaired Student's *t* test. Asterisks are used to denote significance as follows: *, $P < 0.05$, **, $P < 0.01$.

References

Ahuja N., Schwer B., Carobbio S., Waltregny, D., North, B.J., Castronovo, V., Maechler, P., & Verdin E. (2007). Regulation of insulin secretion by SIRT4, a mitochondrial ADP-ribosyltransferase. *J Biol Chem*, 282:33583–33592.

Alsafadi, H.N., Staab-Weijnitz, C.A., Lehmann, M., Lindner, M., Peschel, B., Konigshoff, M., & Wagner, D.E. An ex vivo model to induce early fibrosis-like changes in human precision-cut lung slices. *Am J Physiol Lung Cell Mol Physiol* 312: L896-L902.

Altschul, R., Hoffer, A., & Stephen, J.D. (1955). Influence of nicotinic acid on serum cholesterol in man. *Arch Biochem Biophys*, 54:558–559.

Balan, V., Miller, G.S., Kaplun, L., Balan, K., Chong, Z.Z., Li, F., Kaplun, A., VanBerkum, M.F., Arking, R., & Freeman, D.C. et al. (2008). Life span extension and neuronal cell protection by Drosophila nicotinamidase. *J. Biol. Chem,* 283, 27810–27819.

Belenky, P., Racette, F.G., Bogan, K.L., McClure, J.M., Smith, J.S. & Brenner, C. (2007). Nicotinamide riboside promotes Sir2 silencing and extends lifespan via Nrk and Urh1/Pnp1/Meu1 pathways to NAD. *Cell,* 129,473–484.

Biernacka, A., Dobaczewski, M., & Frangogiannis, N.G. (2011) TGF-β signaling in fibrosis. *Growth Factors* 29(5): 196-202.

Bitterman, K.J., Anderson, R.M., Cohen, H.Y., Latorre-Esteves, M. & Sinclair, D.A. (2002). Inhibition of silencing and accelerated aging by nicotinamide, a putative negative regulator of yeast sir2 and human SIRT1. *J. Biol. Chem*, 277, 45099-45107.

Broustas, C.G. & Lieberman, H.B. (2014) DNA damage response genes and the development of cancer metastasis. *Radiat Res.* 181(2):111-30.

Brown, K.D., Maqsood, S., Huang, J.Y., Pan, Y., Harkcom, W., Li, W., Sauve, A., Verdin, E., & Jaffrey, S.R. (2014) Activation of SIRT3 by the NAD precursor

nicotinamide riboside protects from noise-induced hearing loss. *Cell Metab.,* 20:1059–1068.

Campisi, J. (2013). Aging, cellular senescence, and cancer. *Annu. Rev. Physiol,* 75, 685–705.

Canto, C., Houtkooper, R.H., Pirinen, E., Youn, D.Y., Oosterveer, M.H., Cen, Y., Fernandez-Marcos, P.J., Yamamoto, H., Andreux, P.A., Cettour-Rose, P., Gademann, K., Rinsch, C., Schoonjans, K., Sauve, A.A., & Auwerx, J. (2012). The NAD precursor nicotinamide riboside enhances oxidative metabolism and protects against high-fat diet-induced obesity. *Cell Metab*., 15:838–847.

Collado, M. & Serrano, M. (2010). Senescence in tumours: evidence from mice and humans. *Nat Rev Cancer. 10(1):51-7.*

Connell, N.J., Houtkooper, R.H., & Schrauwen, P. (2019). NAD metabolism as a target for metabolic health: have we found the silver bullet? *Diabetologia,* doi: 10.1007/s00125-019-4831-3.

Coppé, J., Desprez, P., Krtolica, A., & Campisi, J. (2010). The Senescence-Associated Secretory Phenotype: The Dark Side of Tumor Suppression. *Annu Rev Pathol*. 5: 99-118.

Cox T.R., Bird, D., Baker, A., Barker, H.E., Ho, M., Lang, G., & Erler, J.T. (2013). LOX-mediated collagen crosslinking is responsible for fibrosis-enhanced metastasis. *Cancer Res*. 3(6):1721–1732.

D'Amours, D., Desnoyers, S., D'Silva, I., & Poirier, G.G. (1999) Poly(ADP-ribosyl)ation reactions in the regulation of nuclear functions. *Biochem. J*. 342:249–268.

Dai, J.M., Wang, Z.Y., Sun, D.C., Lin, R.X., & Wang, S.Q. (2007). SIRT1 interacts with p73 and suppresses p73-dependent transcriptional activity. *J Cell Physiol*. 210:161–166.

De Jesús-Cortés, H., Xu, P., Drawbridge, J., Estill, S.J., Huntington, P., Tran, S., Britt, J., Tesla, R., Morlock, L., Naidoo, J., Melito, L.M., Wang, G., Williams, N.S., Ready, J.M., McKnight, S.L., & Pieper, A.A. (2012). Neuroprotective efficacy of

aminopropyl carbazoles in a mouse mdel of Parkinson disease. *Proc Natl Acad Sci*, 109(42): 17010-17015.

Duan, F.X., Shi, Y.J., Chen, J., Ding, S.Q., Wang, F.C., Tang, J., Wang, R., Shen, L., Xi, J., Qi, Q., Lü, H.Z., Hu, J.G. (2019). Neuroprotective effects of P7C3 against spinal cord injury in rats. *Exp Biol Med*, 244(18) 1680-1687.

Egeblad, M., Rasch, M.G., & Weaver, V.M. (2010). Dynamic interplay between the collagen scaffold and tumor evolution. *Curr Opin Cell Biol.* 22(5): 687-706.

Eustermann, S., Wu, W., Langelier, M., Yang, J., Easton, L.F., Riccio, A.A., Pascal, J.M., & Neuhaus, D. (2015). Structural Basis of Detection and Signaling of DNA Single-Strand Breaks by Human PARP-1. *Mol Cell* 60(5): 742-754.

Fang, E.F., Scheibye-Knudsen, M., Chua, K.F., Mattson, M.P., Croteau, D.L. & Bohr, V.A. (2016). Nuclear DNA damage signalling to mitochondria in ageing. *Nat Rev Mol Cell Biol,* 17, 308–32.

Fisher, M. (2017). Census and evaluation of p53 target genes. *Oncogene* 36: 3943–3956.

Frye, R.A. (2000). Phylogenetic classification of prokaryotic and eukaryotic Sir2-like proteins. *Res Commun*, 273(2):793-8.

Green, D.R. & Chipuk, J.E. (2006). P53 Metabolism: Inside the TIGAR. *Cell* 126, 30-32.

Gu, C., Zhang, Y., Hu, Q., Wu, J., Ren, H., Liu, C.F., & Wang, G. (2017). P7C3 inhibits GSK3β activation to protect dopamingergic neurons against neurotoxin-induced cell death in vitro and in vivo. *Cell Death Dis*, 8(6): e2858.

Gomes, A.P., Price, N.L., Ling, A.J., Moslehi, J.J., Montgomery, M.K., Rajman, L., White, J.P., Teodoro, J.S., Wrann, C.D., & Hubbard, B.P. et al. (2013). Declining NAD(+) induces a pseudohypoxic state disrupting nuclear-mitochondrial communication during aging. *Cell,* 155, 1624–1638.

Hassa, P.O. & Hottiger, M.O. (2008). The diverse biological roles of mammalian PARPs, a small but powerful family of poly-ADP-ribose polymerases. *Front Biosci* 13:3046-82.

Hershberger, K.A., Martin, A.S., & Hirschey, M.D. (2017). Role of NAD and mitochondrial sirtuins in cardiac and renal diseases. *Nat Rev Nephrol,* 13(4):213-225.

Jeong, S.M., Xiao, C., Finley, L.W., Lahusen, T., Souza, A.L., Pierce, K., Li, Y.H., Wang, X., Laurent, G., German, N.J., Xu, X., Li, C., Wang, R.H., Lee, J., Csibi, A., Cerione, R., Blenis, J., Clish, C.B., Kimmelman, A., Deng, C.X., & Haigis, M.C. (2013). SIRT4 has tumor-suppressive activity and regulates the cellular metabolic response to DNA damage by inhibiting mitochondrial glutamine metabolism. *Cancer Cell,* 23:450–463.

Jiang, R., Zhou, Y., Wang, S., Pang, N., Huang Y., Ye, M., Wan, T., Qiu, Y., Pei, L., Jiang, X., Huang, Y., Yang, H., Ling, W., Li, X., Zhang, Z., & Yang, L. (2019) Nicotinamide riboside protects against liver fibrosis induced CCL4 via regulating the acetylation of Smads signaling pathway. *Life Sci,* 225:20-28.

Kauppinen, T.M. & Swanson, R.A. (2007). The role of poly(ADP-ribose) polymerase-1 in CNS disease. *Neuroscience*, 145:1267-1272.

Kane, A.E. & Sinclair, D.A. (2018). Sirtuins and NAD in the Development and Treatment of Metabolic and Cardiovascular Diseases. *Circ Res,* 123(7):868-885.

Ko, H.L. & Ren, E.C. (2012). Functional aspects of PARP1 in DNA repair and transcription. *Biomolecules* 2:524–548.

Krishnakumar, R. and Kraus, W.L. (2010). The PARP side of the nucleus: molecular actions, physiological outcomes, and clinical targets. *Mol. Cell* 39:8–24.

Kuilman, T. & Peeper, D. S. (2009). Senescence-messaging secretome: SMS-ing cellular stress. *Nature Rev. Cancer,* 9, 81–94.

Kulikova, V., Shabalin, K., Nerinovski, K., Dolle, C., Niere, M., Yakimov, A., Redpath, P., Khodorkovskiy, M., Migaud, M.E., Ziegler, M., & Nikiforov, A. (2015). Generation, release, and uptake of the NAD precursor nicotinic acid riboside by human cells. *J Biol Chem*, 290:27124–27137.

Langley, E., Pearson, M., Faretta, U., Bauer, U.M., Frye, R.A., Minucci, S., Pelicci, P.G. & Kouzarides, T. (2002) Human SIR2 deacetylates p53 and antagonizes PML/p53-induced cellular senescence. *EMBO J*. 21**:**2383-2396.

Lopez-Otın, C., Blasco, M.A., Partridge, L., Serrano, M. & Kroemer, G. (2013). The hallmarks of aging. *Cell,* 153, 1194–1217.

Love, S., Barber, R., & Wilcock, G.A. (1999). Increased poly(ADP-ribosyl)ation of nuclear proteins in Alzheimer's disease. *J. Neurol.*, 122: 247-253.

Mao, Z., Hine, C., Tian, X., Van Meter, M., Au, M., Vaidya, A., Seluanov, A., & Gorbunova, V. (2011). SIRT6 promotes DNA repair under stress by activating PARP1. *Science,* 332:1443–1446.

Meyer, S., Chibly, A.M., Burd, R., & Limesand, K.H. (2017) Insulin-like growth factor-1-mediated DNA repair in irradiated salivary glands is sirtuin-1 dependent. *J Dent Res*. 96:225–232.

Mouchiroud, L., Houtkooper, R.H., Moullan, N., Katsyuba, E., Ryu, D., Canto, C., Mottis, A., Jo, Y.S., Viswanathan, M., Schoonjans, K. et al. (2013). The NAD(+)/Sirtuin pathway modulates longevity through activation of mitochondrial UPR and FOXO signaling. *Cell,* 154, 430–441.

Munoz-Espin, D. & Serrano, M. (2014). Cellular senescence: form physiology to pathology. *Nat Rev Mol Cell Bio,* 15, 482-496.

North, B.J. & Verdin, E. (2007). Interphase nucleo-cytoplasmic shuttling and localization of SIRT2 during mitosis. *PLoSOne,* 2:e784.

Ong, A.L.C & Ramasamy, T.S. (2018). Role of Sirtuin1-p53 regulatory axis in aging, cancer and cellular reprogramming. *Ageing Res Rev*, 43:64–80.

Pacher, P. & Szabó, C. (2005). Role of poly(ADP-ribose) polymerase-1 activation in the pathogenesis of diabetic complications: endothelial dysfunction, as a common underlying theme. *Antioxid. Redox Signaling*, 7: 1568-1580.

Peralta-Leal, A., Rodriguez-Vargas, J.M., Aguilar-Quesada, R., Rodriguez, M.I., Linares, J.L., de Almodovar, M.R., & Oliver, F.J. (2009). PARP inhibitors: new partners in the therapy of cancer and inflammatory diseases. *Free Radical Biol. Med*., 47: 13-26.

Pieper, A.A., McKnight, S.L., & Ready, J.M. (2014). P7C3 and an unbiased approach to drug discovery for neurodegenerative diseases. *Chem Soc Rev*, 43(19): 6716-6726.

Pissios, P. (2017) Nicotinamide N-methyltransferase: more than a vitamin B3 clearance enzyme. *Trends Endocrinol Metab*. 28(5): 340-353.

Pruitt, K., Zinn, R.L., Ohm, J.E., McGarvey, K.M., Kang, S.H., Watkins, D.N., Herman, J.G., & Baylin, S.B. (2006). Inhibition of SIRT1 reactivates silenced cancer genes without loss of promoter DNA hypermethylation. *PLoSGenet*, 2:e40.

Qui, H., Weng, D., Chen, T., Shen, L., Chen, S., Wei, Y., Wu, Q., Zhao, M., Li, Q., Hu, Y., Zhang, Y., Zhou, Y., Su, Y., Zhang, F., Lu, L., Zhou, N., Li, S., Zhang, L., Wang, C., & Li, H. (2017). Stimulator of Interferon Genes Deficiency in Acute Exacerbation of Idiopathic Pulmonary Fibrosis. Front. Immunol. 8(1756).

Ratajczak, J., Joffraud, M., Trammell, S. et al. (2016). NRK1 controls nicotinamide mononucleotide and nicotinamide riboside metabolism in mammalian cells. *Nat Commun* 7, 13103.

Rardin, M.J., He, W., Nishida, Y., Newman, J.C., Carrico, C., Danielson, S.R., Guo, A., Gut, P., Sahu, A.K., Li, B., Uppala, R., Fitch, M., Riiff, T., Zhu, L., Zhou, J., Mulhern, D., Stevens, R.D., Ilkayeva, O.R., Newgard, C.B., Jacobson, M.P., Hellerstein, M., Goetzman, E.S., Gibson, B.W., & Verdin, E. (2013). SIRT5 regulates the mitochondrial lysine succinylome and metabolic networks. *Cell Metab,* 18:920–933.

Revollo, J.R., Grimm, A.A., & Imai, S. (2004). The NAD biosynthesis pathway mediated by Nicotinamide phosphoribosyltransferase regulates Sir2 activity in mammalian cells. *J Biol Chem*, 279(49):50754-63.

Ryu, D., Zhang, H., Ropelle, E.R., Sorrentino, V., Mazala, D.A., Mouchiroud, L., Marshall, P.L., Campbell, M.D., Ali, A.S., Knowels, G.M., Bellemin, S., Iyer, S.R., Wang, X., Gariani, K., Sauve, A.A., Canto, C., Conley, K.E., Walter, L., Lovering, R.M., Chin, E.R., Jasmin, B.K., Marcinek, D.J., Menzies, K.J., & Auwerz, J. (2016). NAD repletion improves muscle function in muscular dystrophy and counters global PARylation. *Sci Transl Med*, 8(362):361ra139.

Rodgers J.T., Lerin C., Haas, W., Gygi S.P., Spiegelman, B.M., & Puigserver, P. (2005). Nutrient control of glucose homeostasis through a complex of PGC-1alpha and SIRT1. *Nature,* 434:113–118.

Schwartz, D. & Rotter, V. (1998) P53-dependent cell cycle control: response to genotoxic stress. *Semin Cancer Biol* 8(5): 325-336.

Straub, J.M., New, J., Hamilton, C.D., Lominska, C., Shnayder, Y., & Thomas, S.M. (2015). Radiation-induced fibrosis: mechanisms and implications for therapy. *J Cancer Res Clin Oncol*, Nov; 141(11): 1985–1994.

Trammell, S.A., Schmidt, M.S., Weidemann, B.J., Redpath, P., Jaksch, F., Dellinger, R.W., Li, Z., Abel, E.D., Miguad, M.E., & Brenner, C. (2016). Nicotinamide riboside is uniquely and orally bioavailable in mice and humans. *Nat Commun,* 7:12948.

Trammell, S.A., Weidemann, B.J., Chadda, A., Yorek, M.S., Holmes, A., Coppey, L.J., Obrosov, A., Kardon, R.H., Yorek, M.A., & Brenner, C. (2016). Nicotinamide Riboside Opposes Type 2 Diabetes and Neuropathy in Mice. *Sci Rep,* 6:26933.

Vaziri, H., Dessain, S.K., Ng Eaton. E., Imai, S.I., Frye, R.A., Pandita, T.K., Guarente, L., & Weinberg, R.A. (2001). hSIR2(SIRT1) functions as an NAD -dependent p53 deacetylase. *Cell,* 107:149–159.

Vijg, J., Dong, X., Milholland, B. & Zhang, L. (2017). Genome instability: a conserved mechanism of ageing? *Essays Biochem,* 61, 305–315.

Walker, A.K., Rivera, P.D., Wang, Q., Chuang, J.C., Tran, S., Osborne-Lawrence, S., Estill, S.J., Starwalt, R., Huntington, P., Morlock, L., Naidoo, J., Williams, N.S., Ready, J.M., Eisch, A.J., Pieper, A.A., & Zigman, J.M. (2015). The P7C3 class of neuroprotective compounds exerts antidepressent efficacy in mice by increasing

hippocampal neurogenesis. *Mol Psychiatry*, 20(4): 500-508.

Wang, G., Han, T., Nijhawan D., Theodoropoulos, P., Naidoo, J., Yadavalli, S., Mirzaei, H., Pieper, A.A., Ready, J.M., & McKnight, S.L. (2014). P7C3 neuroprotective chemicals function by activating the rate-limiting enzyme in NAD salvage. *Cell*, 158(6): 1324-1334.

Wang, S.N., Xu, T.Y., Wang, X., Guan, Y.F., Zhang, S.L., Wang, P., Miao, C.Y. (2016) Neuroprotective Efficacy of an Aminopropyl Carbazole Derivative P7C3-A20 in Ischemic Stroke. *CNS Neurosci Ther*, 22(9): 782-788.

Wei, Y., Kim, T.J., Peng, D.H., Duan, D., Gibbons, D.L., Yamauchi, M., Jackson, J.R., Le Saux, C.J., Calhoun, C., Peters, J., Derynck, R., Backes, B.J., & Chapman, H.A. (2017). Fibroblast-specific inhibition of TGF-β1 signaling attenuates lung and tumor fibrosis. *J Clin Invest.* 127(10): 3675-3688.

Weidele, K., Beneke, S., & Burkle, A. (2017). The NAD precursors nicotinic acid improves genomic integrity in human peripheral blood mononuclear cells after X-irradiation. *DNA repair,* 52:12-12.

Wood, R.D., Mitchell, M., Sgouros, J., & Lindahl, T. (2001). Human DNA Repair Genes. *Science* 291(5507):1284-1289.

Yin, T.C., Britt, J.K., De Jesús-Cortés, H., Lu, Y., Genova, R.M., Khan, M.Z., Voorhees, J.R., Shao, J., Katzman, A.C., Huntington, P.J., Wassink, C., McDaniel, L., Newell, E.A., Dutca, L.M., Naidoo, J., Cui, H., Bassuk, A.G., Harper, M.M., McKnight, S.L., Ready, J.M., Pieper, A.A. (2014). P7C3 neuroprotective chemicals block axonal degeneration and preserve function after traumatic brain injury. *Cell Rep*, 8(6):1731-1740.

Yeung, F., Hoberg, J.E., Ramsey, C.S., Keller, M.D., Jones, D.R., Frye, R.A., & Mayo, M.W. (2004). Modulation of NF-kappaB-dependent transcription and cell survival by the SIRT1deacetylase. *EMBOJ,* 23:2369–2380.

Yoshino, J., Mills, K.F., Yoon, M.J., & Imai, S. (2011). Nicotinamide mononucleotide, a key NAD(+) intermediate, treats the pathophysiology of diet- and age-induced diabetes in mice. *Cell Metab*, 14(4):528-36.

Zha, S., Li, Z., Cao, Q., Wang, F., & Liu, F. (2018). PARP1 inhibitor (PJ34) improves the function of aging-induced enothelial progenitor cells by preserving intracellular NAD levels and increasing SIRT1 activity. *Stem Cell Res Ther,* 9(1):224.

Zhang, Y., Bharathi, S.S., Rardin, M.J., Uppala, R., Verdin, E., Gibson, B.W., & Goetzman, E.S. (2015). SIRT3 and SIRT5 regulate the enzyme activity and cardiolipin binding of very longchain acyl-CoA dehydrogenase. *PLoSOne*, 10:e0122297.

Zhang, Y., Jiang, M., Nouraie, M., Roth, M.G., Tabib, T., Winters, S., Chen, X., Sembrat, J., Chu, Y., Cardenes, N., Tuder, R.M., Herzog, E.L., Ryu, C., Rojas, M., Lafyatis, R., Gibson, K.F., McDyer, J.F., Kass, D.J., & Alder, J.K. (2019). GDF15 is an epithelial-derived biomarker of idiopathic pulmonary fibrosis. *Am J Physiol Lung Cell Mol Physiol*. 317(4):L510-L521.

Zhang, H., Ryu, D., Wu, Y., Gariani, K., Wang, X., Luan, P., D'Amico, D., Ropelle, E.R., Lutolf, M.P., & Aebersold, R. et. al. (2016). NAD(+) repletion improves mitochondrial and stem cell function and enhances life span in mice. *Science,* 352, 1436–1443.

Zhu, X.H., Lu, M., Lee, B.Y., Ugurbil, K. & Chen, W. (2015). In vivo NAD assay reveals the intracellular NAD contents and redox state in healthy human brain and their age dependences. *Proc Natl Acad Sci, USA* 112, 2876–2881.